Contrasting life-history traits of black spruce and jack pine influence their physiological response to drought and growth recovery in northeastern boreal Canada.

William Marchand[1, 2, 3, *], Martin P. Girardin[1, 3], Henrik Hartmann[4], Mathieu Lévesque[5], Sylvie Gauthier[3,1], Yves Bergeron[1,6]

1. Centre d'étude de la forêt, Université du Québec à Montréal, C.P. 8888, succ. Centre-ville, Montréal, QC H3C 3P8, Canada.
2. Department of Forest Ecology, Faculty of Forestry and Wood Sciences, Czech University of Life Sciences Prague, Kamýcká 129, Praha 6 – Suchdol 165 00, Czech Republic
3. Natural Resources Canada, Canadian Forest Service, Laurentian Forestry Centre, 1055 du P.E.P.S, P.O. Box 10380, Stn. Sainte-Foy, Québec, QC G1V 4C7, Canada
4. Max-Planck Institute for Biogeochemistry, Department of Biogeochemical Processes, Hans-Knöll Str. 10, 07745 Jena, Germany
5. Forest Management/Silviculture Group, Institute of Terrestrial Ecosystems, Department of Environmental Systems Science, ETH Zurich, 8092 Zurich, Switzerland.
6. Institut de recherche sur les forêts, Université du Québec en Abitibi-Témiscamingue, 445 boul. de l'Université. Rouyn-Noranda, QC J9X 5E4, Canada

* William Marchand. **Telephone number**: +420 608 391 893; **Email:** william.marchand@uqat.ca

W.M. https://orcid.org/0000-0003-2114-5244

M.P.G. https://orcid.org/0000-0003-0436-7486

H.H. https://orcid.org/0000-0002-9926-5484

M.L. https://orcid.org/0000-0003-0273-510X

S.G. https://orcid.org/0000-0001-6720-0195

Y.B. https://orcid.org/0000-0003-3707-3687

Highlights

- A drop in growth rates of black spruce and jack pine occurred in 1988-1992.
- We tested if growth declines were coupled with changes in tree-ring isotopic signals.
- Drought conditions in 1989 triggered lower $\Delta^{13}C$ and higher $\Delta^{18}O$ values.
- Trees likely closed stomata under a drier climate, reducing their carbon inputs.
- Impacts were higher for spruce, suggesting a low ability to adapt to future climate.

Graphical abstract:

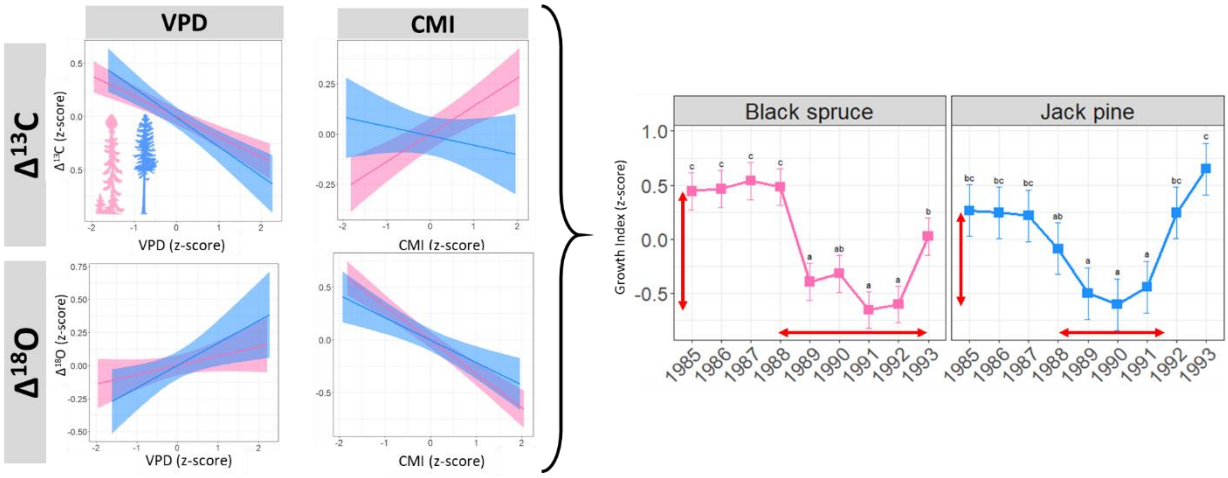

Abstract

An increase in frequency, intensity and duration of drought events affects forested ecosystems. Trees react to these changes by adjusting stomatal conductance to maximize the trade-off between carbon gains and water losses. A better understanding of the consequences of these drought-induced physiological adjustments for tree growth could help inferring future productivity potentials of boreal forests. Here, we used samples from a forest inventory network in Canada where a decline in growth rates of black spruce (*Picea mariana* (Mill.) B.S.P.) and jack pine (*Pinus banksiana* Lamb.) occurred in 1988-1992, an exceptionally dry period, to verify if this growth decline resulted from physiological adjustments of trees to drought. We measured carbon and oxygen isotope ratios in growth rings of 95 spruces and 49 pines spanning 1985-1993. We used ^{13}C discrimination ($\Delta^{13}C$) and ^{18}O enrichment ($\Delta^{18}O$) as proxies for intrinsic water use efficiency and stomatal conductance, respectively. We studied how inter-annual variability in isotopic signals was linked to climate moisture index, vapour pressure deficit and annual snowfall amount. We found significantly lower $\Delta^{13}C$ values over 1988-1990, and significantly higher $\Delta^{18}O$ values in 1988-1989 and 1991 compared to the 1985-1993 averages. We also observed that a low climatic water balance and a high vapor pressure deficit were linked with low $\Delta^{13}C$ and high $\Delta^{18}O$ in the two study species, in parallel with low growth rates. The latter effect persisted into the year following drought for black spruce, but not for jack pine. These findings highlight that small differences in physiological parameters between species could translate into large differences in post-drought recovery. The stronger and longer lasting impact on black spruce compared to jack pine suggests a less efficient carbon use and a lower acclimation potential to future warmer and drier climate conditions.

Key words: boreal forest; dendrochronology; *Picea mariana*; *Pinus banksiana*; tree-ring isotopes; drought stress

Introduction

Earth's surface temperature has increased on average by 1°C since the industrial revolution (i.e. ~ 1850, IPCC (2013)). This is largely the result of a rise in atmospheric CO_2 concentrations caused by the burning of fossil fuels as an anthropogenic energy source (Keeling et al., 2015; Willeit et al., 2019). Global climate models predict an additional warming up to 3°C by the end of the 21st century (IPCC, 2013) that will increase evaporative demand over large parts of the terrestrial surface without being compensated by higher precipitation inputs (Dai, 2013). An increase in the frequency, duration and intensity of climate extremes, such as droughts and heatwaves, is also highly likely (Christidis et al., 2015; Vicente-Serrano et al., 2014). These changes in climate averages, variability and seasonality are already affecting the integrity of natural ecosystems worldwide. Forest ecosystems, for example, can be impacted both directly through water and heat stresses affecting plant physiology (e.g. Grossiord et al., 2020), and indirectly, e.g. via an alteration of disturbance regimes which feed back on mortality rates and regeneration capacity of trees (Adams et al., 2010; Allen et al., 2010; Boucher et al., 2020; Mantgem et al., 2009; Peng et al., 2011). Such hot and dry extremes could severely decrease the productivity of forest biomes over an extended time-period (Restaino et al., 2016; Williams et al., 2013; Yuan et al., 2019). Understanding mechanisms governing the physiological response of trees to extreme drought events is thus of crucial importance for estimating the future C storage capacity of forests.

Inter-annual and long-term changes in tree growth rates are driven in large parts by carbon and water acquisitions which, in turn, are controlled by two major physiological processes: photosynthesis and transpiration. Water acquisition, mainly driven by soil moisture availability, directly influences plant growth by creating turgor pressure which is necessary for wood cells enlargement (Rossi et al., 2009). Water is the main component of xylem sap, which conveys nutrients from roots to leaves (Peel, 2013). Under limited water supply, trees will not use the carbon acquired because of reduced photosynthesis rates and decreased needs for organs elongation (Körner, 2015). Furthermore, photosynthetic enzyme kinetics are temperature-dependent and when temperature increases above a certain threshold, carbon assimilation

rates decrease as a function of soil moisture availability (Kumarathunge et al., 2020; Reich et al., 2018). Trees can buffer these heat stresses by increasing transpiration rates to cool leaf surface, but this is conditional to a sufficient soil moisture availability to cover evaporative demand (Urban et al., 2017). Therefore, the growth performance of a tree is partly governed by a trade-off between maintaining hydraulic integrity and thus slowing down the depletion of water resources via stomatal closure and keeping high carbon gains via stomatal opening (i.e. the "safety-efficiency trade-off"; see Manzoni et al. (2013)). The intensity by which a tree will need to regulate stomatal aperture is largely dependent on the capacity of xylem vessels to resist embolism (Eisenach and Meinzer, 2020; Hacke et al., 2001; Lens et al., 2011; Li et al., 2018). Stomatal regulation is thus the key short-term physiological mechanism by which trees are able to avoid xylem cavitation to survive low atmospheric and soil moisture conditions (Brodribb et al., 2014).

Tree species can be located on a continuous gradient of stomatal regulation on the basis of the strategy used to control plant water potential during a drought, through the notion of isohydricity (Hochberg et al., 2018; Tardieu and Simonneau, 1998). Historically, isohydricity has been viewed as strictly dichotomic, separating plant species between "drought tolerant" and "drought avoider" depending on their propensity to maintain a high hydraulic conductance under dry conditions (Tardieu and Simonneau, 1998). However, results are now accumulating that demonstrate that different species could use different stomatal regulation strategies distributed along a isohydricity continuum (Hartmann et al., 2021; Hochberg et al., 2018; Klein, 2014; Martínez-Vilalta et al., 2014; McDowell et al., 2008). On one hand, some tree species differ from others by closing stomata early when dry conditions occur to maintain their hydraulic function. However, when dry conditions last over an extended period, this high stomatal sensitivity implies a prolonged period without carbon acquisition, which leads to a reduction of non-structural carbohydrate supply. Ultimately, trees from these more isohydric species are at a higher risk of being impacted and killed by biotic agents such as insects, fungus or diseases as a side effect of the lower amount of carbon available for defense mechanisms (McDowell and Sevanto, 2010; Sala et al., 2010). On the other hand, more anisohydric tree species can maintain a high stomatal conductance and very low water potentials under dry

conditions, operating closer to their hydraulic limits. These species keep high carbon assimilation rates at the expense of a high risk of hydraulic failure. This phenomenon occurs because, when soil moisture becomes increasingly scarce, the water column that flows through a xylem conduit tends to break (cavitation) when the tension is too high. As a result, an air bubble, or embolism, forms within the xylem vessel, rendering it unable to conduct water to the leaves (Choat et al., 2018). Hydraulic failure occurs when a too high percentage of conductive vessels are embolized, which could, ultimately, kill the tree (Anderegg et al., 2015a). The stomatal sensitivity of plants, and thus their position along the isohydricity continuum, is varying both in space and time. First, the selection pressure of environmental factors, especially moisture availability, on life-history traits such as the characteristics of conductive vessels and rooting system, drive differences in isohydricity between species (Bhaskar et al., 2007; Feng et al., 2019; Isaac-Renton et al., 2018; McDowell et al., 2019; Wu et al., 2020). Second, the stomatal sensitivity of a species can change depending on inter-annual variations in moisture availability and in drought intensity (Wu et al., 2020). Thus, species more prevalent on mesic sites or xeric sites with cold climates usually exhibit a high stomatal sensitivity in response to low-magnitude changes in their environment. However, these species typically possess more cavitation-resistant xylem vessels (Brodribb et al., 2014) allowing them to maintain only a weak stomatal control under exceptionally dry conditions (Bréda et al., 2006; Li et al., 2018; Wu et al., 2020). By contrast, species growing in more humid environments generally exhibit a more isohydric behaviour but possess xylem vessels more vulnerable to cavitation which force them to apply a very strict stomatal control during extreme droughts (Bréda et al., 2006; Tissier et al., 2004; Wu et al., 2020). These differences in isohydricity between species drive their resistance to and recovery from droughts (Li et al., 2020).

Tree rings record inter-annual changes in physiological processes through variations in the number of annual wood cells, their properties (e.g. cell wall thickness) and chemical composition (e.g. stable isotopes) (see e.g. Babst et al., 2018). In particular, leaf gas exchange drives the ratio of stable carbon and oxygen isotopes that are imprinted in tree-ring biomass (Farquhar et al., 1982a; Gessler et al., 2014). On

the one hand, tree-ring carbon isotope ratio, $\delta^{13}C$, depends on atmosphere-to-tree-ring carbon isotopic discrimination, which is modulated by the leaf to atmosphere CO_2 concentration ratio. Thus, $\delta^{13}C$ is driven by both stomatal conductance and photosynthesis rates (Farquhar et al., 1982b). This relationship makes $\delta^{13}C$ a good proxy for the quantity of carbon a tree assimilates per unit of water transpired, i.e. the intrinsic water use efficiency (iWUE, see Farquhar et al. (1989)). Indeed, tree-ring oxygen isotope ratio, $\delta^{18}O$, partly depends on external influences such as the oxygen isotopic composition of the source water and the enrichment in ^{18}O occurring before water enters the tree hydraulic pathway (Barbour, 2007; Roden et al., 2000). The main tree physiological process directly influencing $\delta^{18}O$ is the control of stomatal aperture, which regulates oxygen isotopic discrimination occurring when water is transpired (Gessler et al., 2014). Other internal processes, such as the "Péclet effect" and the exchange of oxygen atoms between carbohydrates and stem water prior to cellulose formation also act to modify the final $\delta^{18}O$ signal in tree rings (Gessler et al., 2014; Sternberg, 2009), but these processes are not influenced by changes in environmental conditions. $\delta^{18}O$ is often measured in combination with $\delta^{13}C$ to gain a better understanding of past changes in stomatal control that have occurred independently of changes in assimilation rates (i.e. the "dual isotope approach"; Scheidegger et al. (2000)).

Thus, tree rings offer an annually-resolved proxy to study past modifications in trees' physiological processes resulting from environmental changes. For example, during conditions causing stomatal closure but under which trees can maintain high photosynthesis rates, such as short-term droughts and heatwaves, transpiration is reduced while carbon assimilation is still fuelled by the remaining leaf internal CO_2. This lowers the discrimination against the heavier isotopic molecules (i.e. ^{13}C and ^{18}O), leading to less negative $\delta^{13}C$ and $\delta^{18}O$ isotope ratios in growth rings (Cernusak et al., 2013). However, during a long-lasting drought, internal CO_2 concentrations fall below the level required to efficiently fuel photosynthesis, leading to growth rings less depleted in ^{13}C but more enriched in ^{18}O compared with a growth ring formed under average climate conditions (Sternberg, 2009). By contrast, changes in environment can improve photosynthesis and keep non-limiting moisture availability, e.g. after release from overstory competition.

Under these conditions, $\delta^{13}C$ will increase as a result of higher photosynthesis rates whereas $\delta^{18}O$ will show no change compared with growth rings formed under a highly competitive environment.

Here, we used carbon and oxygen isotope composition in tree rings to approximate iWUE and stomatal conductance of jack pine and black spruce growing in non-managed forests of northeastern North America. These two conifer species are broadly distributed and of high commercial value. They occupy contrasting ecological niches and possess highly different life-history traits. Black spruce is a mostly generalist species, growing on a large gradient of soil conditions. This species is particularly well adapted to waterlogged, poorly-drained and organic-rich soils, with a superficial rooting system mostly composed of adventitious structures (Burns and Honkala, 1990). Jack pine occurs mainly on well-drained and sand-rich soils. Its rooting habits include a taproot, allowing access to deep soil water reserves (Burns and Honkala, 1990). These differences lead to contrasting climate sensitivities, black spruce being more negatively affected by exceptionally hot conditions during spring and previous summer compared to jack pine (Marchand et al., 2019). We previously observed a punctual but marked drop in growth rates for these two species within the period 1988-1992 (Girardin et al., 2014; Marchand et al., 2019), and wanted to understand whether carbon and water limitations may have been driving these declines. Here, our main objective was to determine if this growth decline was synchronous with a physiological response of trees to dry and hot extreme conditions that occurred in northeastern Canadian boreal forest. We were particularly interested in determining the extent to which the contrasting life-history traits of black spruce and jack pine influenced their physiological response to drought and the magnitude of the subsequent impacts on growth rates. More specifically, we made the following hypotheses:

(1) In view of previous results for the same species and area, we expect a higher drop in growth rates in spruce compared to pine.

(2) We expect that this drop in growth rates had occurred in parallel with a significant increase in iWUE (decrease in ^{13}C discrimination) and a significant decrease in stomatal conductance (increase in ^{18}O enrichment).

(3) Because jack pine is more abundant on well drained, sandy areas and can access deeper water reserves, this species should exhibit a more anisohydric behavior than black spruce, i.e. we expect a lower inter-annual variability in tree-ring isotope composition of jack pine compared to black spruce.

(4) The variability in isotopic signals should be more strongly linked with moisture conditions in spruce compared to pine because of differences in rooting systems between the two species

Materials and methods

Sampling area

In this study, we took advantage of a provincial forest inventory network in northeastern Canada covering three degrees of latitude and nearly 20 degrees of longitude north of the Quebec limit of commercial forests, i.e. north of 49°N (Létourneau et al., 2008). The territory had recorded in 1989 its highest forest area burned (two million ha; Canadian Forest Service, 2010; Hanes et al., 2018; Soja et al., 2007) within the 1959–2018 period, which is an indication of a severe seasonal drought occurrence during that particular period (Girardin et al., 2014). As part of the forest inventory, 400m^2 circular, randomly distributed, temporary sample plots (TSP; n = 875 plots) were established from 2005 to 2009 within needleleaf-dominated, fire-originating unmanaged forests. These plots encompass a broad gradient of climate conditions, from warm and dry climate at the westernmost locations (mean 1981-2010 temperature and precipitation normals of -1.40°C and 849mm, respectively) to cold climate in the eastern portion of the area (mean 1981-2010 temperature and precipitation normals of -2.17°C and 909mm, respectively). Due to these differences in regional climate, topography and surficial deposits, climatic water balance during the growing season (May-September) is more than two times higher in the eastern than in the western part of the study area (Fig.1). Together with this climate gradient are changes in physiography and soil conditions, from flat terrains composed of organic-rich soils in the west to hillsides composed of tills in the central portion of the territory, to rocky hilltops further east (Robitaille et al., 2015).

Basal Area Increment data

Within each TSP, stem disks were collected for stem analyses from one to three upper canopy trees per species. Disks were prepared and processed for ring-width measurement following standard dendrochronological procedures across four radii per disk (Ministère des Ressources Naturelles du Québec, 2008). Cross-dating and measurements were statistically validated using the program COFECHA (Holmes, 1983). For each stem disk, ring widths of the four radii were averaged and converted to basal area increments ($BAI_t = \pi R^2_t - \pi R^2_{t-1}$; function bai.out of the R package dplR, Bunn (2008)). To remove

biological trends (i.e. those trends arising from increase in tree age and size and from changes in competition pressure with stand development), BAIs were detrended applying generalized additive mixed models (GAMMs). Readers are referred to Marchand et al. (2019) for the detailed statistical procedure (also see Supplementary methods S.1). A growth index, hereafter GI, was then computed as the ratio between observed and predicted BAI values by the GAMMs, for the whole trees' life-period. This is a unit-centered index, i.e. a value below unity means an observed BAI lower than the BAI expected for a tree of a specific age and size and growing under specific environmental conditions. A total of 1,755 spruces and 267 pines that grown during the 1985-1993 time-period were available.

Isotope measurements

A subsample of 144 trees (95 spruces and 49 pines) more than 30 years old and exempt of missing rings were randomly selected for carbon isotope analysis. The sampled trees were randomly chosen among a pool of candidate trees growing on relatively similar conditions, with elevation ranging between 250 m and 550 m a.s.l., organic layer thickness lower than 30 cm, and located on well-drained, sandy or loamy soils. Note that the two species never co-occurred within a TSP among the randomly selected trees. Trees from stands with highly diverse age and diameter structures were avoided to exclude individuals that regenerated by layering and those that have experienced a prolonged period of suppressed growth. The stable oxygen isotope ratio ($\delta^{18}O_{ring}$) was measured for a subset of 53 spruces and 28 pines randomly chosen among the 144 individuals sampled for carbon isotope analysis.

From each stem disk, a 0.8cm x 0.8cm wood strip, from bark to bark and including the pith was cut using a bandsaw. We focused on the year 1989 as an exceptionally dry year. We chose to analyse growth rings formed during the four years directly preceding and following this focal year. This procedure allowed to compare the isotopic signatures between years with average climate conditions and extremely dry and hot years, including the year 1989. This choice also allows to capture any lag (legacy effect) in the physiological response of trees to drought. To do so, annual tree rings covering the period 1985-1993 were individually separated using a scalpel under a binocular microscope. The thinnest rings (ring widths < ~0.1

mm) were separated using a sledge microtome coupled with a digital camera. Rings were ground to fine particles using a Retsch MM400 ball mill. To limit the risk of contamination by plastic particles (Isaac-Renton et al., 2016), we used stainless steel balls and vials during the milling step; coupled with racks allowing to process up to 20 samples per batch. Knowing that isotopic signals of wholewood and α-cellulose of studied species are highly correlated (Bégin et al., 2015; Harlow et al., 2006; Walker et al., 2015), we did not proceed with resin, lignin and hemi-cellulose extractions. We are aware that wholewood leads to additional noise (Gessler et al., 2014), which we can account for when studying the link between isotopic signals and environmental gradients. About 0.3-1.0 mg of the milled wood material was loaded into tin foil capsules and combusted for $\delta^{13}C$ analysis in an elemental analyser (EA 1100, CE Instruments, Milan, Italy) coupled to an IRMS (Delta+, Thermo Finnigan, Bremen, Germany). The analytical precision was ±0.07 ‰ (standard deviation). For $\delta^{18}O$ analysis, about 0.5 mg of wood particles was weighted into silver capsules and pyrolyzed in an elemental analyser (Hekatech-HTO, Wegberg, Germany) coupled to an IRMS (Delta+ XL, Thermo Finnigan, Bremen, Germany). The analytical precision was ±0.14 ‰ (standard deviation). Values are reported in parts per thousand (per mill, ‰), relative to the Vienna Pee Dee Belemnite (VPDB) for carbon ratios and to the Vienna Standard Mean Ocean Water (VSMOW) for oxygen ratios. All isotope measurements were conducted at the Stable Isotope Laboratory (BGC-IsoLab, Max Planck Institute for Biogeochemistry, Jena, Germany). The total number of samples analysed was 1,292 for carbon isotope ratio, and 726 for oxygen isotope ratio.

Corrections for non-climatic variability in tree-ring isotope composition

The $\delta^{13}C_{ring}$ values were converted to ring-to-atmosphere carbon isotope discrimination ($\Delta^{13}C_{ring}$) using Eq.1 in order to account for the decline in $\delta^{13}C$ of atmospheric CO_2 (Suess effect) resulting from the combustion of fossil fuels by human populations since the industrial revolution (Keeling, 1979):

Eq.1

$$\Delta^{13}C_{ring} = \frac{(\delta^{13}C_a - \delta^{13}C_{ring})}{1+\left(\frac{\delta^{13}C_{ring}}{1000}\right)},$$

where $\delta^{13}C_a$ represents the atmospheric stable carbon isotope ratio, obtained from Graven et al. (2017).

Contrary to $\delta^{13}C_{ring}$ that is primarily driven by plant stomatal regulation and carbon assimilation, inter-annual variations in tree-ring $\delta^{18}O$ ($\delta^{18}O_{ring}$) could strongly depend on the oxygen isotope composition of source water (i.e. mainly precipitation) (McCarroll and Loader, 2004), which is in turn related to temperature and atmospheric circulation patterns (Dansgaard, 1964). As we were interested in inter-annual variability in $\delta^{18}O_{ring}$ as a proxy for changes in tree stomatal regulation, it was important to make it free of other time-varying influences. However, we did not have access to measurements of stable oxygen isotope ratio in precipitation ($\delta^{18}O_{prec}$) for our study sites. Instead, we used Eq.2 developed by Barbour et al. (2001):

Eq.2 $$\delta^{18}O_{prec} = 0.52 * T_{mean} - 0.006 * (T_{mean})^2 + 2.42 * P - 1.43 * (P)^2 - 0.46 * \sqrt{Elev.} - 13.00,$$

where T_{mean} is the monthly average temperature (°C), P is the monthly total precipitation (in m) obtained from BioSIM 11 (see below), and *Elev.* is the elevation (m a.s.l.), extracted for our sample plots from the SRTM 90m Digital Elevation Database v4.1 (Jarvis et al., 2008).

Eq.2 was developed based on data from different species (including conifers) and biomes and considers conditions of the specific location (temperature, precipitation and elevation) (Barbour et al., 2001). This equation was used by Guerrieri et al. (2019) to correct tree-ring $\delta^{18}O$ from 12 North American tree species. However, we acknowledge that this formula is not specific to our study area and species. Furthermore, using a single equation for all our locations could thus lead to additional noise in the corrected tree-ring isotopic ratios. To assess the reliability of precipitation $\delta^{18}O$ values estimated using Eq.2, we extracted monthly precipitation $\delta^{18}O$ from three stations close to our study area that are part of the GNIP network (Global Network of Isotopes in Precipitation; Schotterer et al. (1996)): Chapais (49.82 N - 74.97 W), Bonner Lake (49.38 N – 82.12 W) and Goose Bay (53.32 N – 60.42 W). Time series available for these locations spanned the period 1997-2010, and no data was available for our specific time-window. The GNIP data was highly correlated to Eq.2-based precipitation $\delta^{18}O$ (Pearson's R= 0.87, Figure S.2.1). In addition, we extracted monthly precipitation $\delta^{18}O$ from published isoGSM outputs, available for 1985-1993 (Yoshimura et al., 2008). Even if values within the bottom left side of the plot (lower $\delta^{18}O$) are

underestimated (more negative) when based on Eq.2 compared with isoGSM values, these two datasets are also highly correlated (Pearson's R = 0.95, Supplementary Figure S.2.1).

Then, we averaged $\delta^{18}O_{Prec}$ at an annual scale, and calculated the ^{18}O enrichment in tree rings relative to the oxygen isotopic composition of precipitation using Eq.3. By doing so, we assumed that no fractionation occurred before water entered the hydraulic pathway:

Eq.3

$$\Delta^{18}O_{ring} = \frac{(\delta^{18}O_{ring} - \delta^{18}O_{prec})}{1+\left(\frac{\delta^{18}O_{prec}}{1000}\right)}.$$

Despite the high correlation between precipitation $\delta^{18}O$ from isoGSM outputs and values estimated using Eq.2, analyses including isoGSM-corrected $\delta^{18}O$ show different patterns compared with Eq.2-corrected values, especially regarding the relationships between $\Delta^{18}O$ and climate. This could be the result of the relatively coarse resolution of isoGSM model outputs (Yoshimura et al., 2008). In regards of this uncertainty, we decided to show results based on precipitation $\delta^{18}O$ approximated by Eq.2 in the main document, and we provided results based on isoGSM-corrected $\delta^{18}O$ as supplementary information (Figure S.2.2, Table S.2.3).

Climate and environmental variables

BioSIM 11 was used to obtain climate data for our study plots over the period 1985-1993. The BioSIM software provides, for a specific location, elevation-adjusted daily weather estimates interpolated based on historical observations from the four nearest weather stations (Régnière and Bolstad, 1994). Monthly averages of vapour pressure deficit (VPD, in hPa) were derived from this daily data. Summer (June-August) VPD was used as a proxy for atmospheric water demand. Climate moisture index (CMI, in mm) was computed as the difference between monthly precipitation and monthly potential evapotranspiration. Growing season (May-September) CMI was used as a proxy for climatic water balance during the period of the year when trees are physiologically active in our study area. We also extracted the total annual (January-December) snowfall amount (converted to water equivalent, in mm). This variable incorporates

information about inter-annual variability in the length of the growing season as well as in the water input as snow (Gaboriau, 2021).

An approximation of the time-since-fire (TSF) was computed for each plot from the ground-level cambial age of the oldest sampled tree within the plot (obtained from the stem analysis). This variable was used in models to control for changes in growth and physiology related to modifications occurring during stand development (e.g. competition pressure) and in soil parameters (e.g. nutrient availability) through time.

Between-plot differences in environmental conditions were accounted for in the analyses by computing a site fertility index (SI). This index is defined as the average height reached by a dominant undamaged tree at age 50 (measured at breast height, 1.3m); used as a measure of how a tree would, theoretically, perform in regard of a specific set of environmental conditions. SI values were extrapolated to the entire study area based on similarities with the sampled stands in terms of environmental conditions, which include climate, soil surficial deposits, elevation, slope and exposition (Gauthier et al. 2015, also see workflow diagram S.3.1). SI values were available for black spruce only but were also a good indicator for jack pine productivity potential for comparable site conditions (see Supplementary Figure S.3.2).

Statistical procedure

To test for inter-annual differences in GI, $\Delta^{13}C_{ring}$ and $\Delta^{18}O_{ring}$, linear mixed models (LMMs) were fitted, which included z-scores of these variables as response variables, the year of ring formation, the species identity and their interaction as explanatory variables, and the random effect of the tree. Z-score standardization (i.e. mean-centering and dividing each value by the standard deviation of the corresponding individual 9 years time-series) was especially relevant in our case because of the high geographical coverage and the high variability that could be the result of differences in site conditions and individual performances. Post-hoc comparisons between years were performed using the function lsmeans of the R-package emmeans (Lenth, 2021), with a Tukey adjustment for multiple comparisons.

To verify if inter-annual variability in growth rates and tree-ring carbon isotopic discrimination and oxygen enrichment was linked with climate variability, we fitted LMMs by species using the function lme of the R-package nlme (Pinheiro et al., 2019). These models included raw (i.e. non z-scored) GI, $\Delta^{13}C_{ring}$ or $\Delta^{18}O_{ring}$ as response variables, summer VPD, May-September CMI, and annual snowfall as explanatory variables, the random effect of the tree and an error term with a first-order autocorrelation structure. Since climate can affect tree growth of the next growing season, we also included summer VPD and May-September CMI of the year prior to ring formation as explanatory variables. To control for the differences in tree and stand developmental stages and in site conditions, we included the inner-bark basal area of the tree, the minimum time-since-fire, the site fertility index, the 1985-1993 average of growing season CMI and the total basal area of the plot as fixed-effect variables in our models. The inner-bark basal area (BA, in mm^2) is defined here as the sum of BAIs of previous years. This variable was incorporated in models to account for changes in physiology (e.g. drought sensitivity, see Girardin et al., 2012) occurring as a result of the increase in tree size. Hogg (1994) observed that, in Canada, the spatial distribution of vegetation was more closely linked with the CMI than with variables linked with thermal gradients. We thus included the 1985-1993 average of growing season CMI in our models to account for regional differences in climate. The total basal area of the plot was calculated as the sum of basal areas of all individual trees with DBH ≥ 9cm. This value, scaled to m^2/ha, was included in our models to account for differences in competition pressure between plots. Explanatory variables were standardized (centered using the average value of all plots and divided by the corresponding standard deviation) prior to analyses to obtain comparable estimated regression slopes. This standardization procedure also reduced the collinearity (VIFs below 3) among explanatory variables. The structure of the fitted LMMs was:

Eq.4 $$X_{ijt} \sim VPD_{jt} + VPDprev_{jt} + CMI_{jt} + CMIprev_{jt} + Snow_{jt} + CMImean_j + BAstand_j + SI_j + BA_{ijt} + TSF_{jt} + (Tree_{ij}) + corCAR1_{ij} + \varepsilon_{ijt},$$

where X_{ijt} is the response variable (either GI of the year of ring formation (t), $\Delta^{13}C_{ring}$ or $\Delta^{18}O_{ring}$) of a tree i in a plot j at a year t; VPD_{jt} is the summer vapor pressure deficit in a plot j at year t; $VPDprev_{jt}$ is the summer

VPD of the year prior to ring formation in a plot *j* at year *t*; CMI_{jt} is the climate moisture index in a plot *j* at a year *t*; $CMIprev_{jt}$ is the CMI of the year prior to ring formation in a plot *j* at year *t*; $Snow_{jt}$ is the total annual snowfall at a plot *j* at a year *t*; $CMImean_j$ is the 1985-1993 average of growing season CMI at a plot *j*; $BAstand_j$ is the total basal area of a plot *j* scaled to $m^2.Ha^{-1}$ at the time of sampling; SI_j is the site fertility index of the plot *j* at the time of sampling (a time-invariant term); BA_{ijt} is the basal area of a tree *i* at a year *t*; TSF_{jt} is the time elapsed from the last fire for a plot *j* at a year *t*; $Tree_{ij}$ denotes the tree identities; *corCAR1* is the error term with a first-order autocorrelation structure; and ε denotes the residuals of the model. We preferred keeping all explanatory variables in our final models instead of performing a model selection based e.g. on AICc. This was done with the idea of easing the comparison of the significance of fixed terms between different response variables and species. We used AIC scores to test for the importance of a nested random effect (tree nested in plot). Fits of models including the nested random effect were slightly better in the case of black spruce but were worse in the case of jack pine. Additionally, the number of trees per plot was very low (1-3 trees only), so we decided to keep only random effect of tree identities in our models. We also tested for the inclusion of 2-way interactions between temporally invariant fixed-effect variables (SI, mean CMI, stand BA) and time-varying climate data (CMI, VPD, Snow). This did not improve our r-squared values, nor led to significantly lower AIC values compared with models without interaction terms. For this reason, we did not include any interaction terms in our models. One should note that analyses of GI were run on the same subset of trees as those used for the analyses of $\Delta^{13}C_{ring}$ to allow comparison between analyses of growth and isotope ratios.

Normality and homogeneity of variance of residuals were visually assessed, with no deviations from statistical assumptions for linear models. All statistical analyses were performed using the R statistical software version 3.6.0 (R Core Team, 2020).

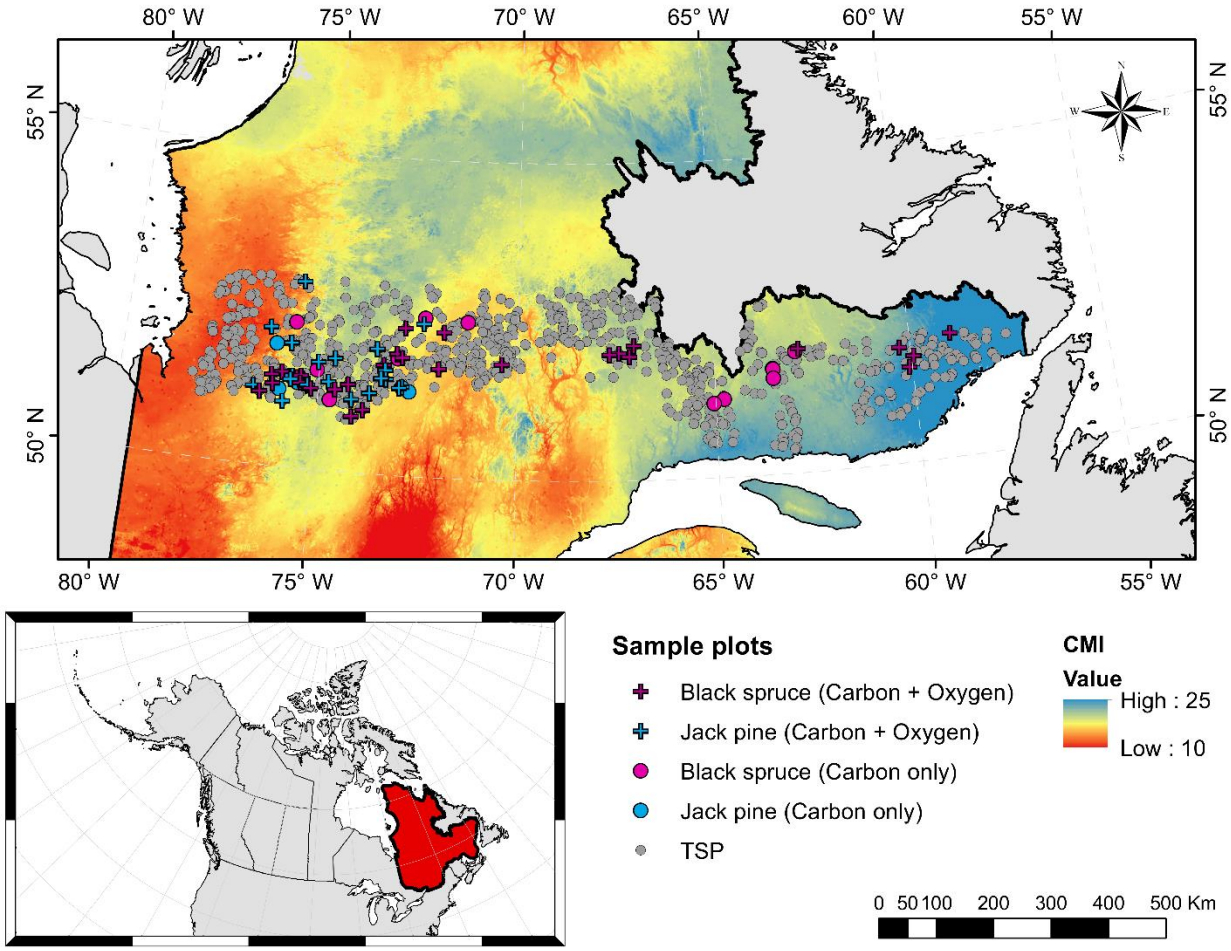

380

381 **Figure 1**: Map of the study area. Color gradient represents the average May-September Climate Moisture
382 Index (CMI, a proxy for the climatic water balance) for the normal period 1981-2010. Symbols represent
383 locations where at least one tree was sampled for isotopic analyses. Coloured circles are for plots where
384 trees were sampled for carbon isotope analysis only, while coloured crosses are for plots where oxygen
385 isotope measurements were also conducted. Pink and blue symbols denote black spruce and jack pine trees,
386 respectively. Grey circles show the locations of the 875 temporary sample plots (TSP) established as part
387 of the Northern Ecoforest Inventory program.

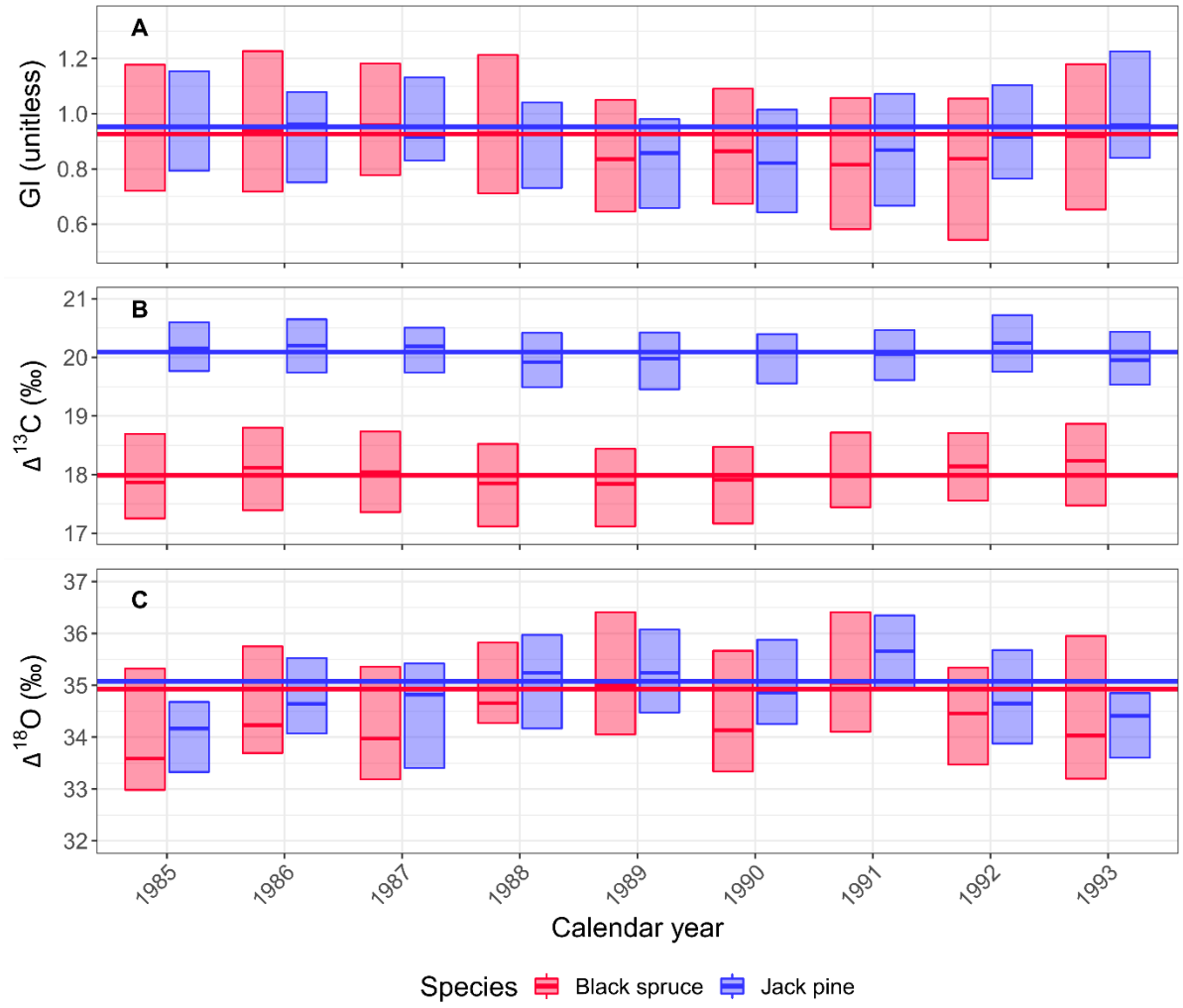

388

389 **Figure 2**: Distribution of observed (i.e. raw) values of the growth index (GI, as the ratio between observed
390 BAI and BAI predicted by the generalized additive mixed models, panel A, see methods), $\Delta^{13}C_{ring}$ (panel
391 B) and $\Delta^{18}O_{ring}$ (panel C), by year and species. The lower and upper hinges of boxplots show the 25th and
392 75th percentiles and the horizontal line denotes median value. Horizontal lines over the whole panel denote
393 1985-1993 averages.

Results

Spatial variability in growth, isotopic signals and climate

Average 1985-1993 BAI was 241 mm^2 for black spruce and 306 mm^2 for jack pine. However, these average growth rates were highly variable between trees and plots, as standard deviations (S.D.) reached ±201.02 mm^2 for black spruce and ±191.29 mm^2 for jack pine. Once variability from biological processes such as tree ageing and demographic processes, and from differences in soil parameters such as thickness of the organic layer, was removed (i.e., after detrending), average growth indices became highly similar between species (Fig. 2). However, standard deviation was still high (0.34 and 0.29 for black spruce and jack pine, respectively). Approximately two third of the trees experienced an average 1985-1993 GI below 1, i.e. an average growth rate lower than the value expected for a tree of similar age and size.

A high variability was also observed in tree-ring isotope data (Fig. 2). For $\Delta^{13}C_{ring}$, the two species exhibited different 1985-1993 carbon discrimination levels, with an average $\Delta^{13}C_{ring}$ of 17.99 ‰ (± 1 ‰) and 20.09 ‰ (± 0.72 ‰) for black spruce and jack pine, respectively. ^{18}O enrichment above source water was of similar magnitude between the two species, with 1985-1993 averages of 34.92 ‰ and 35.09 ‰ for black spruce and jack pine, respectively. However, these values were also highly variable between trees and stands, with S.D. of 2.17 ‰ and 1.69 ‰ for black spruce and jack pine, respectively.

Climate conditions prevailing during 1985-1993 were highly variable depending on the geographic location. Average summer vapor pressure deficit (VPD_{jja}) was higher in the western (6.10 hPa) than in the eastern (3.25 hPa) part of the study area (Fig. 3). In contrast to VPD, climatic water balance during the growing season months did not differ (average May-September CMI of 21.54 and 21.81 mm, in the west and east, respectively). Dates of occurrences of dry extremes also differed between east and west. In the west, trees experienced drier than average water balance (CMI) in 1989 and 1991, whereas in the east, CMI was lower than average in 1988 only. For atmospheric dryness (VPD), both east and west locations experienced dry atmospheric conditions in 1989 and 1991.

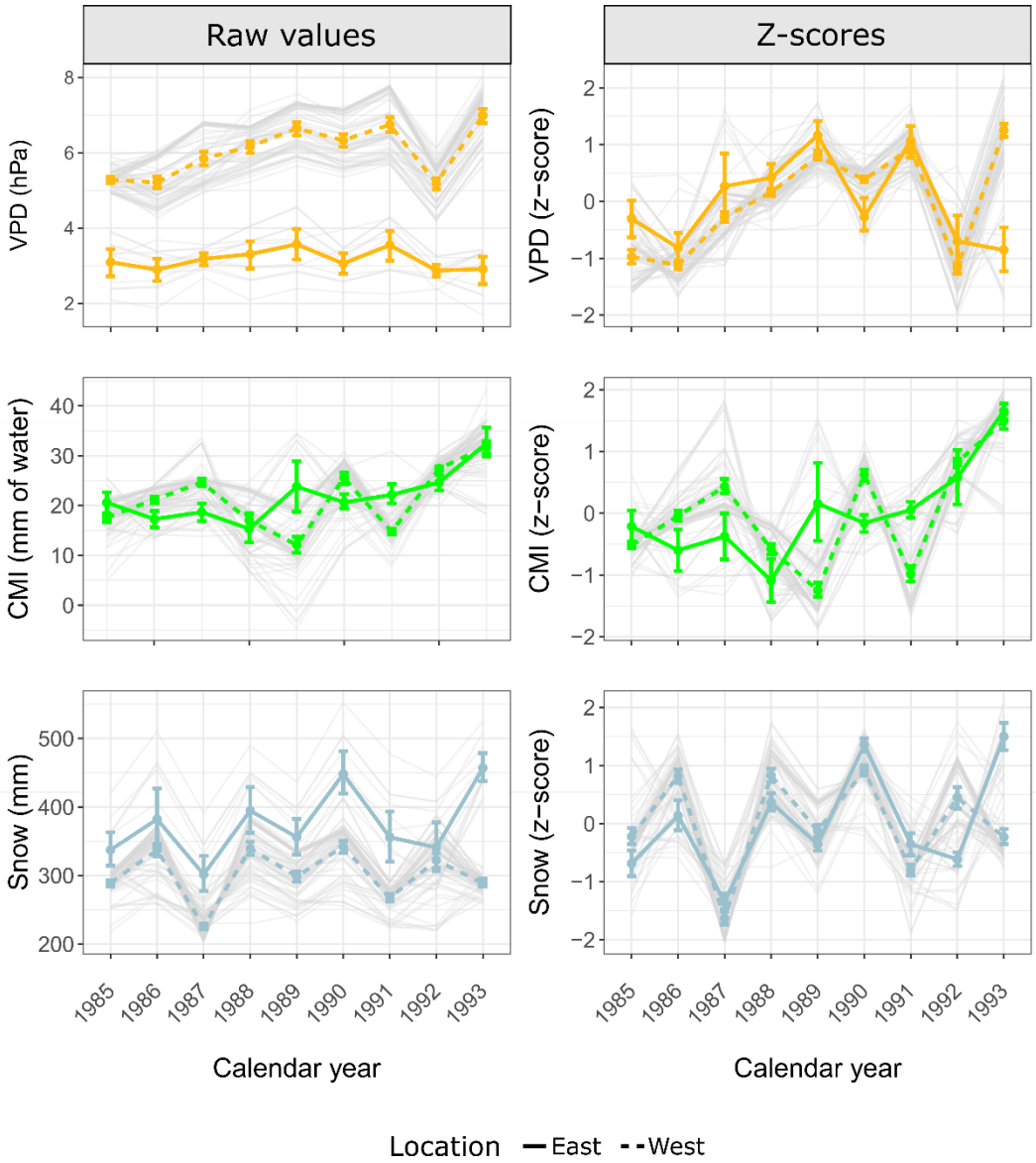

Figure 3: Climate data for the period 1985-1993. Upper panels show summer (June-August) vapor pressure deficit (VPD), middle panels show growing season (May-September) climate moisture index (CMI), lower panels show total annual snowfall. Both raw (left panels) and z-scored (right panels) values are displayed. Dashed lines ("West") display average climate (computed as 50th percentiles of bootstrapped values; 5000 replications) for plots located between 65˚ and 78˚W; solid lines ("East") are for plots located between 58˚ and 65˚W. Error bars are 95% confidence intervals (2.5th and 97.5th percentiles of bootstrapped values). Gray lines indicate time series for each plot location.

Inter-annual differences in growth, carbon and oxygen isotopic signals

When disparities resulting from individual and site-specific differences were removed (i.e. using z-scored values), inter-annual differences in terms of growth rates and isotopic discrimination were emphasized (Fig. 4). In particular, jack pine trees exhibited significantly lower-than-average growth rates during the 1989-1991 period, with least-square means of growth indices being 0.44-0.60 standard deviations (S.D.) below the 1985-1993 average. For black spruce, this slow growth period persisted during the 4-years period 1989-1992, with least-square means of GI 0.32-0.65 S.D. below the 1985-1993 average.

Significant inter-annual differences were also detected in the species-averaged z-scored isotope chronologies (Fig. 4). For black spruce, least-square means of carbon isotopic discrimination were 0.51-0.67 S.D. lower in 1988-1990 compared to the 1985-1993 average, and significantly different from values of adjacent rings. For jack pine the decline in $\Delta^{13}C_{ring}$ was less severe, but the 1988-1990 least-square means were statistically different from 1986-1987 and 1992 values. This pattern was inverted when looking at 1985-1993 least-square means of z-scored iWUE (i.e. higher-than-average iWUE during 1988-1990; Figure S.4.1). Least-square mean of ^{18}O enrichment was the highest in 1991 for both species (0.98 and 1.16 S.D. above the 1985-1993 averages for black spruce and jack pine respectively). Mean of $\Delta^{18}O_{ring}$ was also 0.55-0.60 S.D. higher-than-average in 1988-1989 for black spruce and 0.42 S.D. above the 1985-1993 average in 1989 for jack pine. Interestingly, when looking at the least-square means of $\delta^{18}O$ (non-corrected for precipitation $\delta^{18}O$), 1991 values were still higher than the average value for both species, but 1989 values were not significantly different from or slightly lower than 1985-1993 averages (Figure S.5.1).

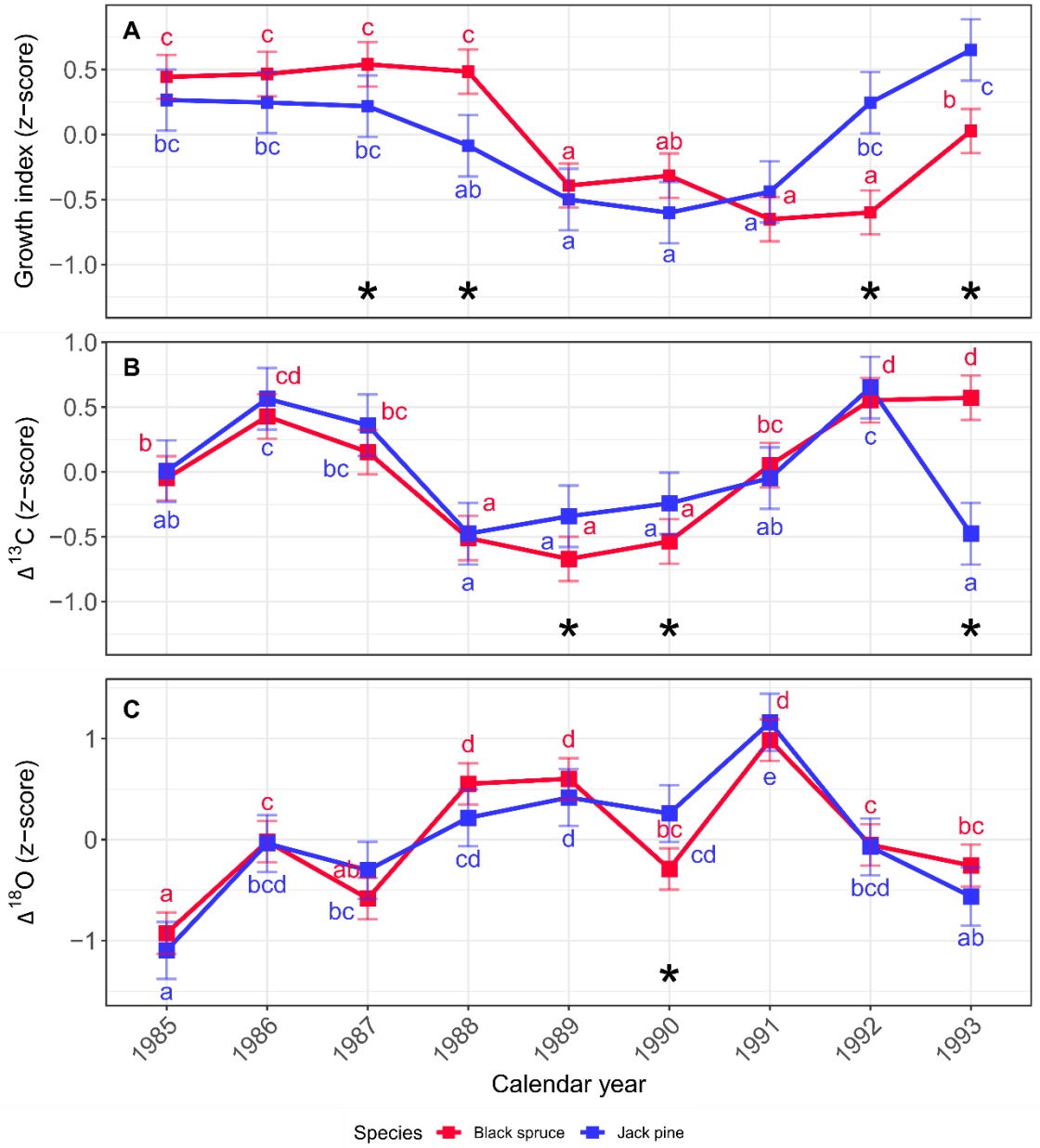

444 **Figure 4**: Z-scored (i.e. the difference between each value and the average value of the individual 1985-
445 1993 series was divided by the standard deviation of the series) growth index (panel A), $\Delta^{13}C$ (panel B)
446 and $\Delta^{18}O$ values (panel C), by year and species. Squares are least square means. Error bars are 95%
447 confidence intervals. For a given variable, different letters indicate significantly different values between
448 years for a given species ($\alpha = 0.05$). Years for which values are significantly different between species are
449 highlighted by an asterisk (*) at the bottom of the panels.

Effect of climate on growth and isotopic signals

High CMI occurring the year of ring formation was linked with significantly higher growth indices (GIs) in both black spruce and jack pine, and a high CMI during the previous growing season was associated with significantly higher GIs in black spruce only (Table 1). Lower black spruce and jack pine GIs were observed when summer VPD occurring the year of ring formation was high, but only black spruce GIs were significantly lower when summer VPD of the year prior to ring formation was high. High snowfall was associated with significantly lower jack pine GIs but with significantly higher black spruce GIs.

The significance of the relationships between climate and isotope discrimination was also species-specific. High summer VPD the year of ring formation was associated with significantly lower carbon isotope discrimination and significantly higher oxygen isotopic enrichment in both species compared to years of low summer VPD (Table 1). The relationship between isotopic values and VPD of the previous summer was similar, but non-significant in the case of jack pine $\Delta^{13}C_{ring}$. A high growing season CMI was linked with significantly higher $\Delta^{13}C_{ring}$ in black spruce only, but significantly lower $\Delta^{18}O_{ring}$ in both species when it occurred the year of ring formation. The significant effect of growing season CMI disappeared when looking at the raw $\delta^{18}O_{ring}$ of pine (Table S.5.2), and at the iWUE of spruce (Table S.4.2). When it occurred the year prior to ring formation, it was linked with higher $\Delta^{18}O_{ring}$ in black spruce, but was not associated with any significant change in jack pine $\Delta^{18}O_{ring}$. A high annual snowfall was linked with significantly lower $\Delta^{13}C_{ring}$ and significantly higher $\Delta^{18}O_{ring}$ in black spruce only, with no significant relationships in the case of jack pine. The effect of snowfall was no longer significant when using black spruce $\delta^{18}O_{ring}$, while this effect switched to significantly positive in the case of jack pine (Table S.5.2). The model outputs also confirmed the high inter-tree variability both in terms of growth rates and isotope ratios, with a very low amount of variance explained by the fixed-effect variables alone (very low marginal r-squared values but high conditional r-squared values, see Table 1).

Table 1 (next page): Results of the linear mixed models of climate effects on tree growth and isotope ratios. One model was fitted by species and response variable, for a total of 6 models. Significant effects are highlighted with gray shadings, with significance levels as follows: " *** " p-value ≤ 0.001; " ** " p-values ≤ 0.01; " * " p-value ≤ 0.05 and " *NS* " indicates non-significant variables. For the random factor, σ^2 is the residual variance, $\tau_{00\ ID\_TREE}$ is the variance explained by the tree identity, and ICC (Interclass Correlation Coefficient) is the ratio between the two metrics and stands for the percent variance explained by the tree identity alone. Also shown the marginal and conditional r-squared, i.e. the percentage of variance explained by the fixed part and the fixed plus random part of the model, respectively; as well as the number of observations (number of rings analysed) and the number of trees. Explanatory variables were mean centered and divided by the corresponding standard-deviation prior to analyses, leading to regression coefficients that are directly comparable with one anothers. Readers are referred to Supporting Information S.6 for a biplot from a principal component analysis (PCA) summarizing results displayed in Table 1.

			Growth Index				$\Delta^{13}C$				$\Delta^{18}O$			
		Predictors	*Estimates*	*std. Error*	*Statistic*	*p*	*Estimates*	*std. Error*	*Statistic*	*p*	*Estimates*	*std. Error*	*Statistic*	*p*
Black spruce	Fixed	Intercept	0.91	0.04	22.46	***	17.85	0.10	175.38	***	35.38	0.33	106.45	***
		CMI	0.02	0.00	3.84	***	0.03	0.01	2.22	*	-0.29	0.04	-7.85	***
		Snow	0.01	0.00	1.96	*	-0.03	0.01	-3.13	**	0.16	0.04	4.21	***
		VPD	-0.02	0.01	-2.27	*	-0.11	0.03	-4.25	***	0.25	0.08	3.11	**
		CMIprev	0.02	0.00	4.85	***	-0.01	0.01	-0.59	NS	0.09	0.04	2.10	*
		VPDprev	-0.04	0.01	-3.19	**	-0.12	0.03	-3.98	***	0.25	0.09	2.87	**
		Stand BA	0.05	0.04	1.17	NS	0.38	0.11	3.53	**	-1.00	0.38	-2.61	*
		mean 1985-1993 CMI	-0.02	0.05	-0.35	NS	-0.06	0.13	-0.48	NS	-0.69	0.40	-1.73	NS
		Size	-0.16	0.05	-3.40	**	-0.01	0.12	-0.05	NS	0.53	0.33	1.60	NS
		Age	0.01	0.04	0.32	NS	0.05	0.10	0.48	NS	-0.56	0.28	-1.97	*
		SI	0.09	0.05	1.86	NS	-0.21	0.12	-1.79	NS	0.22	0.38	0.58	NS
	Random	σ^2	0.03				0.20				0.64			
		$\tau_{00\ ID\_TREE}$	0.11				0.69				4.12			
		ICC	0.78				0.78				0.87			
		N_{ID_TREE}	95				95				53			
		Observations	851				851				475			
		R2 Marginal /Conditional	0.130 / 0.809				0.170 / 0.818				0.173 / 0.889			
Jack pine	Fixed	Intercept	1.08	0.07	16.24	***	20.06	0.14	143.15	***	34.88	0.50	69.65	***
		CMI	0.03	0.01	3.61	***	0.02	0.02	1.13	NS	-0.13	0.06	-2.26	*
		Snow	-0.02	0.01	-2.43	*	-0.02	0.02	-1.13	NS	0.04	0.07	0.58	NS
		VPD	-0.05	0.02	-2.51	*	-0.15	0.03	-4.59	***	0.28	0.13	2.17	*
		CMIprev	0.02	0.01	1.62	NS	-0.02	0.02	-0.86	NS	0.02	0.07	0.26	NS
		VPDprev	-0.01	0.09	-0.13	NS	-0.00	0.04	-0.12	NS	0.35	0.15	2.34	*
		Stand BA	-0.02	0.04	-0.56	NS	-0.34	0.19	-1.77	NS	-0.64	0.75	-0.85	NS
		mean 1985-1993 CMI	-0.01	0.02	-0.51	NS	0.14	0.08	1.68	NS	-0.04	0.28	-0.14	NS
		Size	-0.00	0.05	-0.08	NS	0.02	0.09	0.20	NS	-0.31	0.35	-0.87	NS
		Age	0.18	0.08	2.10	*	0.01	0.18	0.06	NS	0.41	0.57	0.72	NS
		SI	0.01	0.06	0.25	NS	-0.12	0.12	-0.96	NS	-0.26	0.49	-0.53	NS
	Random	σ^2	0.11				0.09				0.84			
		$\tau_{00\ ID\_TREE}$	0.02				0.40				3.08			
		ICC	0.15				0.82				0.79			
		N_{ID_TREE}	49				49				28			
		Observations	441				441				251			
		R2 Marginal /Conditional	0.088 / 0.223				0.143 / 0.849				0.101 / 0.807			

486

Discussion

As expected, we observed a longer-lasting impact of drier-than-average conditions on spruce growth compared to pine. Indeed, two years after the 1991 drought, spruce growth rates barely intersected the 1985-1993 average (i.e. z-score = 0). In contrast, jack pine 1992-1993 growth was higher than the 1985-1993 average and was also higher than spruce growth rates during the same period. This contrasts with the pre-drought period, in which pine had significantly lower growth rates when compared with spruce. When looking at the raw, non-z-scored isotopic ratios, pine displayed significantly higher average $\Delta^{13}C_{ring}$, i.e. lower iWUE, compared with spruce, while no difference was observed in $\Delta^{18}O_{ring}$. This suggests that, instead of different hydraulic behaviours which would have led to higher differences in $\Delta^{18}O_{ring}$, the difference between the two species in terms of $\Delta^{13}C_{ring}$ could originate from different capacities to process carbon uptakes as well as different carbon needs for primary metabolism. Lavigne & Ryan (1997) and Ryan et al. (1997) previously observed a lower carbon use efficiency for black spruce compared to jack pine in the boreal forest of Saskatchewan. These results could indicate that, overall, pine was able to photosynthesize at a higher rate than spruce. When put into the context of adverse climate conditions, this could have allowed pine to recover faster than spruce after the drought. In jack pine, better photosynthesis rates could be related to better N uptakes through access to a larger pool of inorganic N within the mineral soil (Houle et al., 2014).

In line with our second hypothesis, we observed that, during the relatively dry years 1988-1989, $\Delta^{13}C_{ring}$ values were lower and $\Delta^{18}O_{ring}$ values were higher compared to the 1985-1993 averages for both species, and that these changes in isotopic signals paralleled the drop in growth rates, or slightly preceded it in the case of spruce (Fig. 4). As expected, these deviations from 1985-1993 averages isotopic ratios were also lower for pine compared with spruce. According to the conceptual model of Scheidegger et al. (2000), this suggests that trees have closed stomata more intensely during the dry period than before and after these adverse years. This more stringent stomatal regulation could have also induced changes in photosynthesis rates, but we were unable to detect them using isotopic signatures measured in the bulk wood material (i.e.

using a mixture of both earlywood and latewood). Defoliation by insects, such as spruce budworm (*Choristoneura fumiferana* (Clemens)), could induce changes in the water and carbon budgets of trees which could potentially influence the ^{13}C and ^{18}O signals in tree rings. More specifically, such defoliation event could be followed by a period of increased photosynthetic rates through a compensatory mechanism in trees, which would translate into a temporary increase in iWUE (Simard et al., 2008). However, to our knowledge, no insect epidemics occurred within our sampling area over the study period (Ols et al., 2018). A potential explanation for the synchrony in inter-annual variability of isotopic signals and growth rates could be a modification in carbon allocation strategy of trees to reduce secondary stem and root growth (Way and Sage, 2008) and preferentially save and invest in Non-Structural Carbohydrates (NSC) reserves (Hartmann et al., 2015). However, we did not measure NSC concentrations in our samples, so this interpretation remains speculative. Extended drought could also have led to a sustained decrease in photosynthetic rates and, consequently, may have entailed carbon limitation to sink activity. This phenomenon, the lack of available carbon to invest in stem growth and storage, could explain the legacy effect observed in spruce. In view of the markedly more abrupt increase in iWUE (drop in $\Delta^{13}C_{ring}$) for spruce compared to pine, those changes could have been more drastic for this species. Indeed, Way & Sage (2008) found that black spruce seedlings grown at elevated temperature experienced up to 60% lower growth rates compared to seedlings at ambient temperature because of a heat- and drought-induced reduction in cell expansion and division (i.e. limitation of C investment, decrease in the activity of metabolic sinks). This decreases the need of carbon for xylogenesis and instead allows trees to store carbon in the form of starch and sugars (Balducci et al., 2013; Muller et al., 2011; Way and Sage, 2008). Since jack pine is more frequently encountered on sandy areas prone to drying, the species may exhibit a more anisohydric behaviour, which may explain the absence of a significant increase in $\Delta^{18}O_{ring}$ for this species in 1988-1989. This gas-exchange strategy could have also allowed pine trees to store a larger amount of NSC which were then remobilized for growth when water availability was no longer limiting, likely explaining the better recovery of jack pine compared with spruce. In 1991, tree-ring $\Delta^{18}O_{ring}$ significantly increased for both species and this was not mirrored by any change in $\Delta^{13}C_{ring}$. This pattern can be explained by a decrease in

538 assimilation rates that paralleled the decrease in stomatal conductance (Scheidegger et al., 2000), maybe
539 the result of a more stringent regulation of stomatal aperture which significantly lowered carbon uptake.

540 As hypothesized, results from the linear mixed models show that an increase in summer vapour pressure
541 deficit significantly decreased carbon isotope discrimination and increased oxygen enrichment of black
542 spruce and jack pine. Furthermore, growing season CMI had only a marginally significant positive effect
543 on black spruce carbon discrimination but a highly significant negative effect on oxygen isotopic ratios of
544 both species. This latter effect was especially high in the case of black spruce. Because of a shallow,
545 adventitious rooting system, black spruce trees have limited access to deep groundwater sources and use
546 almost exclusively surficial soil water storage. Organic matter is more prone to drying during severe and
547 prolonged droughts compared to mineral soil, which could also explain the higher sensitivity of spruces
548 $\Delta^{18}O_{ring}$ to soil moisture availability compared to pines. These findings suggest that spruce trees close
549 stomata more stringently compared to pine when atmosphere and soil conditions become increasingly dry
550 to save water and maintain their hydraulic integrity. This is not surprising since tree species inhabiting
551 wetter environments, such as black spruce, generally show a lower resistance to embolism and likely have
552 narrower safety margins than species more specific to dry environments such as jack pine (Choat et al.,
553 2012; Wu et al., 2020). Additionally, black spruce reduces the root to shoot ratio as a response to an increase
554 in temperature, which exacerbates the negative impacts of droughts by lowering the capacity of trees to
555 access water (Way and Sage, 2008). Thus, carbon assimilation rates of spruce could have declined early
556 during drought (Adams et al., 2017). A higher rate of cavitated vessels could make this species particularly
557 prone to a so-called “legacy” or “lag” effect in which a dry event induces low growth rates not only the
558 year it occurs but also several years later (Anderegg et al., 2015b; Huang et al., 2018). This was observed
559 here through the significant negative effect of summer VPD and positive effect of growing season CMI of
560 the year prior to ring formation on black spruce growth (Table 1 and Supplementary Figure S.6).
561 Interestingly, we did not observe any statistically significant lag effect for jack pine.

562 We observed a significant effect of total annual snowfall on black spruce growth, carbon and oxygen
563 isotope ratios. Black spruce growth indices were generally higher in regions and years characterized by
564 high annual snowfall, which means that trees had growth rates higher than or closer to those expected under
565 average climate conditions. The corresponding growth rings were more depleted in ^{13}C and enriched in ^{18}O
566 than rings from years and regions with low annual snowfall. In jack pine, annual snowfall had a significant,
567 negative effect on growth indices only. In years and regions characterized by a more abundant annual
568 snowfall, snowmelt and soil thawing can occur late in the season; which can delay the start of growth
569 (Vaganov et al., 1999; Verbyla, 2015). This, linked with an earlier spring budburst in pine compared with
570 spruce (Man et al., 2015), is a likely explanation for the opposite effect of annual snowfall on growth of the
571 two species. For black spruce, an additional snowpack can have helped to protect the shallow root system
572 of trees (Frey, 1983) as well as the newly formed buds (Marquis et al., 2020), which would have outbalanced
573 the negative effect of a delayed soil thaw and growth onset. For this species, the significant effect of annual
574 snowfall observed on $\Delta^{13}C_{ring}$ and $\Delta^{18}O_{ring}$ was opposite in direction to the effect of soil moisture availability
575 and vapor pressure deficit (i.e. $\Delta^{13}C_{ring}$ decreased and $\Delta^{18}O_{ring}$ increased with high snowfall, and with high
576 VPD and low CMI during summer, Table 1, Supplementary Figure S.6). This is likely an indication of
577 hydric stress, as already stated by Walker et al. (2015) in Alaska for the same species. This could also be
578 the result of a higher proportion of wood cells formed during the summer season. More summer-formed
579 cells would lead to a stronger summer drought signal compared to growth rings whose initiation started
580 early in spring. It is interesting to note that, for spruce, the effect of snow was no longer present when
581 looking at $\delta^{18}O_{ring}$ (raw, non-corrected) values (Supplementary Table S.5.2). This is because the $\delta^{18}O$
582 signature in tree rings is likely a mixing between the signal from source water (snow water and water from
583 deeper soil layers is usually more depleted in ^{18}O compared with rainwater and water from soil layers closer
584 to the surface) and the enrichment occurring after water entered the trees hydraulic pathway.

585 Besides the effects of climate variables on $\Delta^{13}C_{ring}$ and $\Delta^{18}O_{ring}$, we observed a high inter-tree variability
586 on isotopic signatures. This becomes particularly apparent through the high variability associated with tree

identity in LMMs, coupled with far higher conditional r-squared than marginal r-squared values. We hypothesize that such variability results from the high spatial heterogeneity in growth conditions. First, climate averages differed within the study zone. Easternmost locations were, on average, more humid than westernmost plots (Fig.1 and 3); and this could have influenced the impact of a below-average summer aridity on trees physiology. Additionally, the intensity of 1988-1989 and 1991 droughts differed between the study plots. Some plots did not experience drier-than-average conditions during these years (Fig. 3). Second, some types of substrates, such as poorly weathered (i.e. relatively young, mainly rocky substrate with no or thin organic horizon) and dry soils (Raney et al., 2016; Sniderhan et al., 2020; Sniderhan and Baltzer, 2016), could exert a long-term impact on tree growth and physiology. Permafrost thaw leading to moisture deficit in the superficial soil layer was invoked by Sniderhan & Baltzer (2016) and Sniderhan et al. (2020) to explain negative growth trends and increasing iWUE of southern black spruce populations within Northwestern Canada. In our case, there is a possibility that the effect of differences in moisture availability occurred at the scale of the micro-environment (i.e. variations in topography and soil conditions within the plot), even if we constrained the selection of trees to relatively similar soil conditions. Competition for water, light and nutrients also decreases the capacity of trees to physiologically react and adapt to fast and episodic changes in their environment (Sohn et al., 2016, 2014, 2012). Those tree populations subjected to such a prolonged stress, including a drier regional climate, can thus be more sensitive to short-term stressors such as droughts (Levanič et al., 2011; Raney et al., 2016). By contrast, some microenvironments, referred to as "hydrological [micro]refugia", buffer the impacts of droughts on trees because of an enhanced capacity to maintain soil water availability under dry conditions (McLaughlin et al., 2017; Stralberg et al., 2020). Our climate dataset, and more generally gridded and interpolated climate datasets, often do not accurately estimate differences in microenvironmental conditions and in groundwater depth, another factor influencing tree-ring isotope signals (Sun et al., 2018). A high inter-tree variability in isotopic signals was previously observed in *Picea mariana* trees in the same geographic area by Bégin et al. (2015) and was attributed to variations in environmental conditions surrounding each individual tree. Differences in rooting depth of trees and genetically-driven differences in trees' physiological status could

613 also contribute to this high inter-tree variability in isotopic ratios (Konter et al., 2014; McCarroll and
614 Loader, 2004). Such differently performing genotypes are linked with diverging forcing factors on the
615 selection of life-history traits. Indeed, environmental gradients, such as differences in regional climate and
616 photoperiod, can influence the genetic structure of trees (McKown et al., 2014) and more specifically their
617 hydraulic traits (Depardieu et al., 2020; Isaac-Renton et al., 2018; Li et al., 2018).

618 Oxygen isotopic signals in tree rings are strongly dependent on the composition of source water.
619 Even if we tried to estimate and remove oxygen isotopic composition of precipitation (Eq.2), the estimated
620 values may not be fully representative of the interannual variability in precipitation ^{18}O that have occurred
621 in the study locations. This highlights the need for a densification of the network of in-situ measurements
622 of isotope composition in precipitation, especially in Eastern Canada where locations with available time-
623 series of precipitation $\delta^{18}O$ are extremely scarce. Such network could be especially useful to overcome the
624 uncertainties when interpreting results from $\delta^{18}O$, such as those we observed here (see Supporting
625 information S.2). Furthermore, additional non-physiological mechanisms could have been involved in the
626 inter-annual differences in $\Delta^{18}O_{ring}$. First, the taproot of jack pine (Burns and Honkala, 1990) makes this
627 species more responsive than superficially-rooted black spruce to deep soil water sources, especially when
628 comparing jack pine with lowland black spruce (Girardin et al., 2008). During years characterized by lower
629 than average surficial soil water supply, jack pine trees could have relied more from deep soil water pools
630 which are usually characterized by a lower ^{18}O enrichment compared with water from soil layers closer to
631 the surface (Tang and Feng, 2001). This could have occurred during the year 1989, for which raw $\delta^{18}O_{ring}$
632 of pine significantly dropped below the 1985-1993 average (Fig. S.5). Further, we analysed isotopic
633 signature of the whole ring, which represents a measure integrated over the entire growing season. So, we
634 were unable to distinguish changes in $\Delta^{18}O_{ring}$ occurring as a result of a modification in the seasonality of
635 precipitation (Xu et al., 2020). Finally, black spruce and jack pine individuals sampled in this study never
636 co-occurred within a sample plot. Even if we cannot fully exclude an effect of environmental and site
637 conditions on the sensitivity of trees to drought, we are confident that the differences we observed here are,

638 at least partly, driven by a differential physiological response between the two species. First, we selected
639 trees on sites with relatively similar drainage conditions, so our analyses did not include spruce trees from
640 clayey or organic soils. Additionally, differences in inter-annual variability of growth index and isotopic
641 signals were analysed by computing least square means on z-scored values (Fig.4). Doing this
642 standardization removes part of the noise in data at the site and individual level, such as the variability
643 induced by different soil conditions or different genotypes. Finally, when linear mixed models were re-run
644 using these z-scored values, between-species differences in the effects of climate on responses variables
645 were still present (Supplementary Table S.7), especially in the case of isotopic signals.

646 To summarize, we identified species-specific recovery capacity from dry conditions using tree-ring
647 isotopic signatures for two boreal conifers. The capacity to recover from a past drought differed between
648 black spruce and jack pine, this divergence being driven by differences in the physiological responses of
649 the studied species. More specifically, we observed a delayed but longer lasting and stronger negative
650 impact of drought on growth rates in black spruce compared to jack pine. A decline in growth rates occurred
651 in parallel with a significant increase in iWUE (decrease in ^{13}C discrimination) and a significant decrease
652 in stomatal conductance (increase in ^{18}O enrichment). Such variations were more significantly linked with
653 moisture conditions in spruce compared to pine, likely mirroring the species' differences in life-history
654 traits (e.g. rooting systems). Together with other morpho-physiological adaptations to a stressful,
655 waterlogged and cold environment (Burns and Honkala, 1990), black spruce exhibits a low acclimation
656 potential to warmer temperatures (Way and Sage, 2008). Taken together, these findings suggest that spruce
657 will be more negatively impacted by droughts and heatwaves than jack pine; with a slower and less
658 complete recovery and a more marked lag effect, as observed here. We recognised that inferring
659 physiological variables from tree-ring isotopic composition, which are measures integrated over the full
660 length of the growing season and the whole tree canopy, likely induced some uncertainties in the estimated
661 effects of climate. Without more direct and finer-resolution proxies of physiological parameters and C-
662 storage status of trees, it is difficult to determine the origin of the observed inter-annual variability in tree-

ring isotopic ratios. A high inter-individual variability in ^{13}C and ^{18}O isotopic signatures was observed, which could be related to contrasting microsite conditions instead of to differences in physiological response to climate. However, this high heterogeneity may also suggest that some of the studied tree populations are better adapted and can better acclimate to warmer and drier conditions than others (Girardin et al., 2021), whereas some areas could also protect trees against negative impacts of warming (Stralberg et al., 2020). Future studies should expand to datasets including plots with co-occurring species to address this uncertainty. Since the difference in post-drought growth rates was visible in growth indices, such variability in post-drought performance between species should be the result of both different ecological niches and life-history traits. Results in this direction would tend to confirm the vulnerability of black spruce populations to future climate warming, as more frequent and more severe drought episodes are anticipated for this region (Chaste et al., 2019; Girardin et al., 2016).

Data availability statement

Data that support the results of this study are available on Figshare (10.6084/m9.figshare.14695404). Weather data are also freely accessible through the BioSIM server (https://cfs.nrcan.gc.ca/projects/133). All relevant software and R functions that were used in this paper are referred to in the "Materials and methods" section (see package vignettes for details). Custom codes for analyses and main figures are available on Figshare (10.6084/m9.figshare.14695404).

Acknowledgements

This study was made possible thanks to the financial support that was provided by the Strategic and Discovery Grant programs of NSERC (Natural Sciences and Engineering Research Council of Canada), doctoral and travel scholarships funded by FRQNT (B2X and international internship programs), and a MITACS scholarship cofunded by Ouranos. Additional financial support was provided by the Centre for Forest Research (Centre d'Étude de la Forêt, CEF), the Canadian Forest Service, the UQAM Foundation (De Sève Foundation fellowship and TEMBEC forest ecology fellowship) and the Quebec Ministère de l'économie, de la Science et de l'innovation (programme PSR-SllRl). We thank Rémi Saint-Amant (Canadian Forest Service) for providing helpful advices on the use of BioSIM software. We are very grateful to Marie Moulin, David Gervais and Christine Simard for the huge help with the processing of wood samples. Many thanks to Xiao Jing Guo (Canadian Forest Service) for helpful advice during statistical analyses, to Savoyane Lambert, Heike Geilmann and Iris Kuhlmann (Max Planck Institute for Biogeochemistry) for isotope measurements, to Fabio Gennaretti (UQAT) for helpful comments on an earlier version of the manuscript, and to Martine Savard, Joëlle Marion, Lauriane Dinis, Joëlle Berthier, Claude Durocher, Marie-Claude Gros-Louis, Philippe Labrie, Alexis Achim, Étienne Boucher, Nathalie Isabel, Claire Depardieu, and Mathilde Pau for help and advice with the processing of wood samples. Finally, we thank the two anonymous reviewers for their constructive comments on an earlier draft of this paper.

Literature cited

Adams, H.D., Macalady, A.K., Breshears, D.D., Allen, C.D., Stephenson, N.L., Saleska, S.R., Huxman, T.E., McDowell, N.G., 2010. Climate-induced tree mortality: earth system consequences. Eos, Transactions American Geophysical Union 91, 153–154. https://doi.org/10.1029/2010EO170003

Adams, H.D., Zeppel, M.J.B., Anderegg, W.R.L., Hartmann, H., Landhäusser, S.M., Tissue, D.T., Huxman, T.E., Hudson, P.J., Franz, T.E., Allen, C.D., Anderegg, L.D.L., Barron-Gafford, G.A., Beerling, D.J., Breshears, D.D., Brodribb, T.J., Bugmann, H., Cobb, R.C., Collins, A.D., Dickman, L.T., Duan, H., Ewers, B.E., Galiano, L., Galvez, D.A., Garcia-Forner, N., Gaylord, M.L., Germino, M.J., Gessler, A., Hacke, U.G., Hakamada, R., Hector, A., Jenkins, M.W., Kane, J.M., Kolb, T.E., Law, D.J., Lewis, J.D., Limousin, J.-M., Love, D.M., Macalady, A.K., Martínez-Vilalta, J., Mencuccini, M., Mitchell, P.J., Muss, J.D., O'Brien, M.J., O'Grady, A.P., Pangle, R.E., Pinkard, E.A., Piper, F.I., Plaut, J.A., Pockman, W.T., Quirk, J., Reinhardt, K., Ripullone, F., Ryan, M.G., Sala, A., Sevanto, S., Sperry, J.S., Vargas, R., Vennetier, M., Way, D.A., Xu, C., Yepez, E.A., McDowell, N.G., 2017. A multi-species synthesis of physiological mechanisms in drought-induced tree mortality. Nat. Ecol. Evol. 1, 1285–1291. https://doi.org/10.1038/s41559-017-0248-x

Allen, C.D., Macalady, A.K., Chenchouni, H., Bachelet, D., McDowell, N., Vennetier, M., Kitzberger, T., Rigling, A., Breshears, D.D., Hogg, E.H. (Ted), Gonzalez, P., Fensham, R., Zhang, Z., Castro, J., Demidova, N., Lim, J.H., Allard, G., Running, S.W., Semerci, A., Cobb, N., 2010. A global overview of drought and heat-induced tree mortality reveals emerging climate change risks for forests. For. Ecol. Manage. 259, 660–684. https://doi.org/10.1016/j.foreco.2009.09.001

Anderegg, W.R.L., Flint, A., Huang, C., Flint, L., Berry, J.A., Davis, F.W., Sperry, J.S., Field, C.B., 2015a. Tree mortality predicted from drought-induced vascular damage. Nat. Geosci. 8, 367–371. https://doi.org/10.1038/ngeo2400

Anderegg, W.R.L., Schwalm, C., Biondi, F., Camarero, J.J., Koch, G., Litvak, M., Ogle, K., Shaw, J.D., Shevliakova, E., Williams, A.P., Wolf, A., Ziaco, E., Pacala, S., 2015b. Pervasive drought legacies in forest ecosystems and their implications for carbon cycle models. Science 349, 528–532. https://doi.org/10.1126/science.aab1833

Babst, F., Bodesheim, P., Charney, N., Friend, A.D., Girardin, M.P., Klesse, S., Moore, D.J.P., Seftigen, K., Björklund, J., Bouriaud, O., Dawson, A., DeRose, R.J., Dietze, M.C., Eckes, A.H., Enquist, B., Frank, D.C., Mahecha, M.D., Poulter, B., Record, S., Trouet, V., Turton, R.H., Zhang, Z., Evans, M.E.K., 2018. When tree rings go global: Challenges and opportunities for retro- and prospective insight. Quat. Sci. Rev. 197, 1–20. https://doi.org/10.1016/j.quascirev.2018.07.009

Balducci, L., Deslauriers, A., Giovannelli, A., Rossi, S., Rathgeber, C.B.K., 2013. Effects of temperature and water deficit on cambial activity and woody ring features in *Picea mariana* saplings. Tree Physiol 33, 1006–1017. https://doi.org/10.1093/treephys/tpt073

Barbour, M.M., 2007. Stable oxygen isotope composition of plant tissue: a review. Functional Plant Biol. 34, 83–94. https://doi.org/10.1071/FP06228

Barbour, M.M., Andrews, T.J., Farquhar, G.D., 2001. Correlations between oxygen isotope ratios of wood constituents of Quercus and Pinus samples from around the world. Functional Plant Biol. 28, 335–348. https://doi.org/10.1071/pp00083

Bégin, C., Gingras, M., Savard, M.M., Marion, J., Nicault, A., Bégin, Y., 2015. Assessing tree-ring carbon and oxygen stable isotopes for climate reconstruction in the Canadian northeastern boreal forest. Palaeogeography, Palaeoclimatology, Palaeoecology 423, 91–101. https://doi.org/10.1016/j.palaeo.2015.01.021

742 Bhaskar, R., Valiente-Banuet, A., Ackerly, D.D., 2007. Evolution of hydraulic traits in closely related
743 species pairs from mediterranean and nonmediterranean environments of North America. New
744 Phytol. 176, 718–726. https://doi.org/10.1111/j.1469-8137.2007.02208.x
745 Boucher, D., Gauthier, S., Thiffault, N., Marchand, W., Girardin, M., Urli, M., 2020. How climate change
746 might affect tree regeneration following fire at northern latitudes: a review. New Forests 51,
747 543–571. https://doi.org/10.1007/s11056-019-09745-6
748 Bréda, N., Huc, R., Granier, A., Dreyer, E., 2006. Temperate forest trees and stands under severe
749 drought: a review of ecophysiological responses, adaptation processes and long-term
750 consequences. Ann. For. Sci. 63, 625–644. https://doi.org/10.1051/forest:2006042
751 Brodribb, T.J., McAdam, S.A.M., Jordan, G.J., Martins, S.C.V., 2014. Conifer species adapt to low-rainfall
752 climates by following one of two divergent pathways. Proc. Natl. Acad. Sci. U.S.A. 111, 14489–
753 14493. https://doi.org/10.1073/pnas.1407930111
754 Bunn, A.G., 2008. A dendrochronology program library in R (dplR). Dendrochronologia 26, 115–124.
755 https://doi.org/10.1016/j.dendro.2008.01.002
756 Burns, R.M., Honkala, B.H., 1990. Silvics of North America: Volume 1. Conifers. United States
757 Department of Agriculture (USDA), Forest Service, Agriculture Handbook 654.
758 Canadian Forest Service, 2010. National Fire Database - Agency Fire Data. Natural Resources Canada,
759 Canadian Forest Service, Northern Forestry Centre., Edmonton, AB.
760 Cernusak, L.A., Ubierna, N., Winter, K., Holtum, J.A.M., Marshall, J.D., Farquhar, G.D., 2013.
761 Environmental and physiological determinants of carbon isotope discrimination in terrestrial
762 plants. New Phytol. 200, 950–965. https://doi.org/10.1111/nph.12423
763 Chaste, E., Girardin, M.P., Kaplan, J.O., Bergeron, Y., Hély, C., 2019. Increases in heat-induced tree
764 mortality could drive reductions of biomass resources in Canada's managed boreal forest.
765 Landscape Ecol 34, 403–426. https://doi.org/10.1007/s10980-019-00780-4
766 Choat, B., Brodribb, T.J., Brodersen, C.R., Duursma, R.A., López, R., Medlyn, B.E., 2018. Triggers of tree
767 mortality under drought. Nature 558, 531–539. https://doi.org/10.1038/s41586-018-0240-x
768 Choat, B., Jansen, S., Brodribb, T.J., Cochard, H., Delzon, S., Bhaskar, R., Bucci, S.J., Feild, T.S., Gleason,
769 S.M., Hacke, U.G., Jacobsen, A.L., Lens, F., Maherali, H., Martínez-Vilalta, J., Mayr, S.,
770 Mencuccini, M., Mitchell, P.J., Nardini, A., Pittermann, J., Pratt, R.B., Sperry, J.S., Westoby, M.,
771 Wright, I.J., Zanne, A.E., 2012. Global convergence in the vulnerability of forests to drought.
772 Nature 491, 752–755. https://doi.org/10.1038/nature11688
773 Christidis, N., Jones, G.S., Stott, P.A., 2015. Dramatically increasing chance of extremely hot summers
774 since the 2003 European heatwave. Nat Clim Chang 5, 46–50.
775 https://doi.org/10.1038/nclimate2468
776 Dai, A., 2013. Increasing drought under global warming in observations and models. Nat Clim Chang 3,
777 52–58. https://doi.org/10.1038/nclimate1633
778 Dansgaard, W., 1964. Stable isotopes in precipitation. Tellus 16, 436–468.
779 https://doi.org/10.1111/j.2153-3490.1964.tb00181.x
780 Depardieu, C., Girardin, M.P., Nadeau, S., Lenz, P., Bousquet, J., Isabel, N., 2020. Adaptive genetic
781 variation to drought in a widely distributed conifer suggests a potential for increasing forest
782 resilience in a drying climate. New Phytol. 227, 427–439. https://doi.org/10.1111/nph.16551
783 Eisenach, C., Meinzer, F.C., 2020. Hydraulics of woody plants. Plant Cell Environ. 43, 529–531.
784 https://doi.org/10.1111/pce.13715
785 Farquhar, G.D., Ball, M.C., von Caemmerer, S., Roksandic, Z., 1982a. Effect of salinity and humidity on
786 $\delta^{13}C$ value of halophytes—Evidence for diffusional isotope fractionation determined by the ratio
787 of intercellular/atmospheric partial pressure of CO_2 under different environmental conditions.
788 Oecologia 52, 121–124. https://doi.org/10.1007/BF00349020

789 Farquhar, G.D., Hubick, K.T., Condon, A.G., Richards, R.A., 1989. Carbon Isotope Fractionation and Plant
790 Water-Use Efficiency, in: Rundel, P.W., Ehleringer, J.R., Nagy, K.A. (Eds.), Stable Isotopes in
791 Ecological Research, Ecological Studies. Springer, New York, NY, pp. 21–40.
792 https://doi.org/10.1007/978-1-4612-3498-2_2
793 Farquhar, G.D., O'Leary, M.H., Berry, J.A., 1982b. On the relationship between carbon isotope
794 discrimination and the intercellular carbon dioxide concentration in leaves. Functional Plant Biol.
795 9, 121–137. https://doi.org/10.1071/pp9820121
796 Feng, X., Ackerly, D.D., Dawson, T.E., Manzoni, S., McLaughlin, B., Skelton, R.P., Vico, G., Weitz, A.P.,
797 Thompson, S.E., 2019. Beyond isohydricity: The role of environmental variability in determining
798 plant drought responses. Plant Cell Environ. 42, 1104–1111. https://doi.org/10.1111/pce.13486
799 Frey, W., 1983. The influence of snow on growth and survival of planted trees. Arct. Antarct. Alp. Res.
800 15, 241–251. https://doi.org/10.1080/00040851.1983.12004347
801 Gaboriau, D., 2021. Régimes des feux holocène, contemporain et futur aux Territoires du Nord-Ouest
802 (Canada) (Ph.D. thesis). UQAM - Université de Montpellier.
803 Gauthier, S., Raulier, F., Ouzennou, H., Saucier, J.-P., 2015. Strategic analysis of forest vulnerability to risk
804 related to fire: an example from the coniferous boreal forest of Quebec. Can. J. For. Res. 45,
805 553–565. https://doi.org/10.1139/cjfr-2014-0125
806 Gessler, A., Ferrio, J.P., Hommel, R., Treydte, K., Werner, R.A., Monson, R.K., 2014. Stable isotopes in
807 tree rings: towards a mechanistic understanding of isotope fractionation and mixing processes
808 from the leaves to the wood. Tree Physiol. 34, 796–818.
809 https://doi.org/10.1093/treephys/tpu040
810 Girardin, M.P., Bouriaud, O., Hogg, E.H., Kurz, W., Zimmermann, N.E., Metsaranta, J.M., Jong, R. de,
811 Frank, D.C., Esper, J., Büntgen, U., Guo, X.J., Bhatti, J., 2016. No growth stimulation of Canada's
812 boreal forest under half-century of combined warming and CO_2 fertilization. Proc. Natl. Acad.
813 Sci. U.S.A. 113, E8406–E8414. https://doi.org/10.1073/pnas.1610156113
814 Girardin, M.P., Guo, X.J., Bernier, P.Y., Raulier, F., Gauthier, S., 2012. Changes in growth of pristine
815 boreal North American forests from 1950 to 2005 driven by landscape demographics and
816 species traits. Biogeosciences 9, 2523–2536. https://doi.org/10.5194/bg-9-2523-2012
817 Girardin, M.P., Guo, X.J., De Jong, R., Kinnard, C., Bernier, P., Raulier, F., 2014. Unusual forest growth
818 decline in boreal North America covaries with the retreat of Arctic sea ice. Glob. Change Biol. 20,
819 851–866. https://doi.org/10.1111/gcb.12400
820 Girardin, M.P., Isabel, N., Guo, X.J., Lamothe, M., Duchesne, I., Lenz, P., 2021. Annual aboveground
821 carbon uptake enhancements from assisted gene flow in boreal black spruce forests are not
822 long-lasting. Nature Communications 12, 1169. https://doi.org/10.1038/s41467-021-21222-3
823 Girardin, M.P., Raulier, F., Bernier, P.Y., Tardif, J.C., 2008. Response of tree growth to a changing climate
824 in boreal central Canada: A comparison of empirical, process-based, and hybrid modelling
825 approaches. Ecol Modell 213, 209–228. https://doi.org/10.1016/j.ecolmodel.2007.12.010
826 Graven, H., Allison, C.E., Etheridge, D.M., Hammer, S., Keeling, R.F., Levin, I., Meijer, H.A.J., Rubino, M.,
827 Tans, P.P., Trudinger, C.M., Vaughn, B.H., White, J.W.C., 2017. Compiled records of carbon
828 isotopes in atmospheric CO_2 for historical simulations in CMIP6. Geoscientific Model
829 Development 10, 4405–4417. https://doi.org/10.5194/gmd-10-4405-2017
830 Grossiord, C., Buckley, T.N., Cernusak, L.A., Novick, K.A., Poulter, B., Siegwolf, R.T.W., Sperry, J.S.,
831 McDowell, N.G., 2020. Plant responses to rising vapor pressure deficit. New Phytologist 226,
832 1550–1566. https://doi.org/10.1111/nph.16485
833 Guerrieri, R., Belmecheri, S., Ollinger, S.V., Asbjornsen, H., Jennings, K., Xiao, J., Stocker, B.D., Martin, M.,
834 Hollinger, D.Y., Bracho-Garrillo, R., Clark, K., Dore, S., Kolb, T., Munger, J.W., Novick, K.,
835 Richardson, A.D., 2019. Disentangling the role of photosynthesis and stomatal conductance on

836 rising forest water-use efficiency. Proc. Natl. Acad. Sci. U.S.A. 201905912.
837 https://doi.org/10.1073/pnas.1905912116
838 Hacke, U.G., Sperry, J.S., Pockman, W.T., Davis, S.D., McCulloh, K.A., 2001. Trends in wood density and
839 structure are linked to prevention of xylem implosion by negative pressure. Oecologia 126, 457–
840 461. https://doi.org/10.1007/s004420100628
841 Hanes, C.C., Wang, X., Jain, P., Parisien, M.-A., Little, J.M., Flannigan, M.D., 2018. Fire-regime changes in
842 Canada over the last half century. Can. J. For. Res. 49, 256–269. https://doi.org/10.1139/cjfr-
843 2018-0293
844 Harlow, B.A., Marshall, J.D., Robinson, A.P., 2006. A multi-species comparison of $\delta^{13}C$ from whole wood,
845 extractive-free wood and holocellulose. Tree Physiol 26, 767–774.
846 https://doi.org/10.1093/treephys/26.6.767
847 Hartmann, H., Link, R.M., Schuldt, B., 2021. A whole-plant perspective of isohydry: stem-level support
848 for leaf-level plant water regulation. Tree Physiology. https://doi.org/10.1093/treephys/tpab011
849 Hartmann, H., McDowell, N.G., Trumbore, S., 2015. Allocation to carbon storage pools in Norway spruce
850 saplings under drought and low CO_2. Tree Physiol. 35, 243–252.
851 https://doi.org/10.1093/treephys/tpv019
852 Hochberg, U., Rockwell, F.E., Holbrook, N.M., Cochard, H., 2018. Iso/anisohydry: a plant–environment
853 interaction rather than a simple hydraulic trait. Trends Plant Sci. 23, 112–120.
854 https://doi.org/10.1016/j.tplants.2017.11.002
855 Hogg, E.H. (Ted), 1994. Climate and the southern limit of the western Canadian boreal forest. Canadian
856 Journal of Forest Research. https://doi.org/10.1139/x94-237
857 Holmes, R.L., 1983. Computer assisted quality control in tree-ring dating and measurement.
858 Houle, D., Moore, J.-D., Ouimet, R., Marty, C., 2014. Tree species partition N uptake by soil depth in
859 boreal forests. Ecology 95, 1127–1133. https://doi.org/10.1890/14-0191.1
860 Huang, M., Wang, X., Keenan, T.F., Piao, S., 2018. Drought timing influences the legacy of tree growth
861 recovery. Glob Chang Biol 24, 3546–3559. https://doi.org/10.1111/gcb.14294
862 IPCC, 2013. Climate Change 2013: The physical science basis. Cambridge University Press, Cambridge,
863 UK.
864 Isaac-Renton, M., Montwé, D., Hamann, A., Spiecker, H., Cherubini, P., Treydte, K., 2018. Northern forest
865 tree populations are physiologically maladapted to drought. Nat. Commun. 9, 1–9.
866 https://doi.org/10.1038/s41467-018-07701-0
867 Isaac-Renton, M., Schneider, L., Treydte, K., 2016. Contamination risk of stable isotope samples during
868 milling. Rapid Commun. Mass Spectrom. 30, 1513–1522. https://doi.org/10.1002/rcm.7585
869 Jarvis, A., Reuter, H., Nelson, A., Guevara, E., 2008. Hole-filled seamless SRTM data v4.
870 Keeling, C.D., 1979. The Suess effect: ^{13}Carbon-^{14}Carbon interrelations. Environ Int 2, 229–300.
871 https://doi.org/10.1016/0160-4120(79)90005-9
872 Keeling, R.F., Walker, S.J., Piper, S.C., Bollenbacher, A.F., 2015. Monthly atmospheric CO_2 concentration
873 data (1958 to present) derived from in-situ air measurements at Mauna Loa Observatory, Hawaii
874 [WWW Document]. URL http://www.scrippsco2.ucsd.edu/
875 Klein, T., 2014. The variability of stomatal sensitivity to leaf water potential across tree species indicates
876 a continuum between isohydric and anisohydric behaviours. Funct. Ecol. 28, 1313–1320.
877 https://doi.org/10.1111/1365-2435.12289
878 Konter, O., Holzkämper, S., Helle, G., Büntgen, U., Saurer, M., Esper, J., 2014. Climate sensitivity and
879 parameter coherency in annually resolved $\delta^{13}C$ and $\delta^{18}O$ from *Pinus uncinata* tree-ring data in
880 the Spanish Pyrenees. Chem. Geol. 377, 12–19. https://doi.org/10.1016/j.chemgeo.2014.03.021
881 Körner, C., 2015. Paradigm shift in plant growth control. Curr. Opin. Plant Biol. 25, 107–114.
882 https://doi.org/10.1016/j.pbi.2015.05.003

883 Kumarathunge, D.P., Drake, J.E., Tjoelker, M.G., López, R., Pfautsch, S., Vårhammar, A., Medlyn, B.E.,
884 2020. The temperature optima for tree seedling photosynthesis and growth depend on water
885 inputs. Glob Chang Biol 26, 2544–2560. https://doi.org/10.1111/gcb.14975
886 Lavigne, M.B., Ryan, M.G., 1997. Growth and maintenance respiration rates of aspen, black spruce and
887 jack pine stems at northern and southern BOREAS sites. Tree Physiol 17, 543–551.
888 https://doi.org/10.1093/treephys/17.8-9.543
889 Lens, F., Sperry, J.S., Christman, M.A., Choat, B., Rabaey, D., Jansen, S., 2011. Testing hypotheses that
890 link wood anatomy to cavitation resistance and hydraulic conductivity in the genus *Acer*. New
891 Phytol. 190, 709–723. https://doi.org/10.1111/j.1469-8137.2010.03518.x
892 Lenth, R.V., 2021. emmeans: Estimated Marginal Means, aka Least-Squares Means. R package version
893 1.5.4.
894 Létourneau, J.P., Matejek, S., Morneau, C., Robitaille, A., Roméo, T., Brunelle, J., Leboeuf, A., 2008.
895 Norme de cartographie écoforestière du Programme d'inventaire écoforestier nordique.
896 Ministère des Ressources naturelles et de la Faune du Québec, Québec.
897 Levanič, T., Čater, M., McDowell, N.G., 2011. Associations between growth, wood anatomy, carbon
898 isotope discrimination and mortality in a *Quercus robur* forest. Tree Physiol. 31, 298–308.
899 https://doi.org/10.1093/treephys/tpq111
900 Li, X., Blackman, C.J., Choat, B., Duursma, R.A., Rymer, P.D., Medlyn, B.E., Tissue, D.T., 2018. Tree
901 hydraulic traits are coordinated and strongly linked to climate-of-origin across a rainfall gradient.
902 Plant Cell Environ. 41, 646–660. https://doi.org/10.1111/pce.13129
903 Li, X., Piao, S., Wang, K., Wang, X., Wang, T., Ciais, P., Chen, A., Lian, X., Peng, S., Peñuelas, J., 2020.
904 Temporal trade-off between gymnosperm resistance and resilience increases forest sensitivity
905 to extreme drought. Nat. Ecol. Evol. 1–9. https://doi.org/10.1038/s41559-020-1217-3
906 Man, R., Colombo, S., Lu, P., Dang, Q.-L., 2015. Effects of winter warming on cold hardiness and spring
907 budbreak of four boreal conifers. Botany. https://doi.org/10.1139/cjb-2015-0181
908 Mantgem, P.J. van, Stephenson, N.L., Byrne, J.C., Daniels, L.D., Franklin, J.F., Fulé, P.Z., Harmon, M.E.,
909 Larson, A.J., Smith, J.M., Taylor, A.H., Veblen, T.T., 2009. Widespread increase of tree mortality
910 rates in the western United States. Science 323, 521–524.
911 https://doi.org/10.1126/science.1165000
912 Manzoni, S., Vico, G., Katul, G., Palmroth, S., Jackson, R.B., Porporato, A., 2013. Hydraulic limits on
913 maximum plant transpiration and the emergence of the safety–efficiency trade-off. New Phytol.
914 198, 169–178. https://doi.org/10.1111/nph.12126
915 Marchand, W., Girardin, M.P., Hartmann, H., Gauthier, S., Bergeron, Y., 2019. Taxonomy, together with
916 ontogeny and growing conditions, drives needleleaf species' sensitivity to climate in boreal
917 North America. Glob. Chang. Biol. 25, 2793–2809. https://doi.org/10.1111/gcb.14665
918 Marquis, B., Bergeron, Y., Simard, M., Tremblay, F., 2020. Growing-season frost is a better predictor of
919 tree growth than mean annual temperature in boreal mixedwood forest plantations. Global
920 Change Biology n/a. https://doi.org/10.1111/gcb.15327
921 Martínez-Vilalta, J., Poyatos, R., Aguadé, D., Retana, J., Mencuccini, M., 2014. A new look at water
922 transport regulation in plants. New Phytol. 204, 105–115. https://doi.org/10.1111/nph.12912
923 McCarroll, D., Loader, N.J., 2004. Stable isotopes in tree rings. Quat. Sci. Rev. 23, 771–801.
924 https://doi.org/10.1016/j.quascirev.2003.06.017
925 McDowell, N., Pockman, W.T., Allen, C.D., Breshears, D.D., Cobb, N., Kolb, T., Plaut, J., Sperry, J., West,
926 A., Williams, D.G., Yepez, E.A., 2008. Mechanisms of plant survival and mortality during drought:
927 why do some plants survive while others succumb to drought? New Phytol. 178, 719–739.
928 https://doi.org/10.1111/j.1469-8137.2008.02436.x
929 McDowell, N.G., Grossiord, C., Adams, H.D., Pinzón-Navarro, S., Mackay, D.S., Breshears, D.D., Allen,
930 C.D., Borrego, I., Dickman, L.T., Collins, A., Gaylord, M., McBranch, N., Pockman, W.T., Vilagrosa,

A., Aukema, B., Goodsman, D., Xu, C., 2019. Mechanisms of a coniferous woodland persistence under drought and heat. Environ. Res. Lett. 14, 045014. https://doi.org/10.1088/1748-9326/ab0921

McDowell, N.G., Sevanto, S., 2010. The mechanisms of carbon starvation: how, when, or does it even occur at all? New Phytol. 186, 264–266. https://doi.org/10.1111/j.1469-8137.2010.03232.x

McKown, A.D., Guy, R.D., Klápště, J., Geraldes, A., Friedmann, M., Cronk, Q.C.B., El-Kassaby, Y.A., Mansfield, S.D., Douglas, C.J., 2014. Geographical and environmental gradients shape phenotypic trait variation and genetic structure in *Populus trichocarpa*. New Phytol. 201, 1263–1276. https://doi.org/10.1111/nph.12601

McLaughlin, B.C., Ackerly, D.D., Klos, P.Z., Natali, J., Dawson, T.E., Thompson, S.E., 2017. Hydrologic refugia, plants, and climate change. Glob Chang Biol 23, 2941–2961. https://doi.org/10.1111/gcb.13629

Ministère des Ressources Naturelles du Québec, 2008. Norme d'inventaire écodendrométrique nordique. Direction des inventaires forestiers, Québec (Province).

Muller, B., Pantin, F., Genard, M., Turc, O., Freixes, S., Piques, M., Gibon, Y., 2011. Water deficits uncouple growth from photosynthesis, increase C content, and modify the relationships between C and growth in sink organs. J. Exp. Bot. 62, 1715–1729.

Ols, C., Girardin, M.P., Hofgaard, A., Bergeron, Y., Drobyshev, I., 2018. Monitoring Climate Sensitivity Shifts in Tree-Rings of Eastern Boreal North America Using Model-Data Comparison. Ecosystems 21, 1042–1057. https://doi.org/10.1007/s10021-017-0203-3

Peel, A.J., 2013. Transport of nutrients in plants. Elsevier, Butterworth-Heinemann, Oxford, UK.

Peng, C., Ma, Z., Lei, X., Zhu, Q., Chen, H., Wang, W., Liu, S., Li, W., Fang, X., Zhou, X., 2011. A drought-induced pervasive increase in tree mortality across Canada's boreal forests. Nat Clim Chang 1, 467–471. https://doi.org/10.1038/nclimate1293

Pinheiro, J., Bates, D., DebRoy, S., Sarkar, D., Heisterkamp, S., Van Willigen, B., R Core Team, 2019. nlme: Linear and Nonlinear Mixed Effects Models.

R Core Team, 2020. R: A language and environment for statistical computing. R Foundation for Statistical Computing, Vienna, Austria.

Raney, P.A., Leopold, D.J., Dovciak, M., Beier, C.M., 2016. Hydrologic position mediates sensitivity of tree growth to climate: Groundwater subsidies provide a thermal buffer effect in wetlands. For Ecol Manag 379, 70–80. https://doi.org/10.1016/j.foreco.2016.08.004

Régnière, J., Bolstad, P., 1994. Statistical simulation of daily air temperature patterns eastern North America to forecast seasonal events in insect pest management. Environ Entomol 23, 1368–1380. https://doi.org/10.1093/ee/23.6.1368

Reich, P.B., Sendall, K.M., Stefanski, A., Rich, R.L., Hobbie, S.E., Montgomery, R.A., 2018. Effects of climate warming on photosynthesis in boreal tree species depend on soil moisture. Nature 562, 263–267. https://doi.org/10.1038/s41586-018-0582-4

Restaino, C.M., Peterson, D.L., Littell, J., 2016. Increased water deficit decreases Douglas fir growth throughout western US forests. Proc. Natl. Acad. Sci. U.S.A. 113, 9557–9562. https://doi.org/10.1073/pnas.1602384113

Robitaille, A., Saucier, J.-P., Chabot, M., Côté, D., Boudreault, C., 2015. An approach for assessing suitability for forest management based on constraints of the physical environment at a regional scale. Can. J. For. Res. 45, 529–539. https://doi.org/10.1139/cjfr-2014-0338

Roden, J.S., Lin, G., Ehleringer, J.R., 2000. A mechanistic model for interpretation of hydrogen and oxygen isotope ratios in tree-ring cellulose. Geochimica et Cosmochimica Acta 64, 21–35. https://doi.org/10.1016/S0016-7037(99)00195-7

977 Rossi, S., Simard, S., Rathgeber, C.B.K., Deslauriers, A., De Zan, C., 2009. Effects of a 20-day-long dry
978 period on cambial and apical meristem growth in *Abies balsamea* seedlings. Trees 23, 85–93.
979 https://doi.org/10.1007/s00468-008-0257-0
980 Ryan, M.G., Lavigne, M.B., Gower, S.T., 1997. Annual carbon cost of autotrophic respiration in boreal
981 forest ecosystems in relation to species and climate. J. Geophys. Res. Atmos. 102, 28871–28883.
982 https://doi.org/10.1029/97JD01236
983 Sala, A., Piper, F., Hoch, G., 2010. Physiological mechanisms of drought-induced tree mortality are far
984 from being resolved. New Phytol. 186, 274–281. https://doi.org/10.1111/j.1469-
985 8137.2009.03167.x
986 Scheidegger, Y., Saurer, M., Bahn, M., Siegwolf, R., 2000. Linking stable oxygen and carbon isotopes with
987 stomatal conductance and photosynthetic capacity: a conceptual model. Oecologia 125, 350–
988 357. https://doi.org/10.1007/s004420000466
989 Schotterer, U., Oldfield, F., Froehlich, K., 1996. GNIP. Global Network for Isotopes in Precipitation.
990 Simard, S., Elhani, S., Morin, H., Krause, C., Cherubini, P., 2008. Carbon and oxygen stable isotopes from
991 tree-rings to identify spruce budworm outbreaks in the boreal forest of Québec. Chemical
992 Geology, Stable Isotope Analysis of Tree Rings 252, 80–87.
993 https://doi.org/10.1016/j.chemgeo.2008.01.018
994 Sniderhan, A.E., Baltzer, J.L., 2016. Growth dynamics of black spruce (Picea mariana) in a rapidly thawing
995 discontinuous permafrost peatland. Journal of Geophysical Research: Biogeosciences 121, 2988–
996 3000. https://doi.org/10.1002/2016JG003528
997 Sniderhan, A.E., Mamet, S.D., Baltzer, J.L., 2020. Non-uniform growth dynamics of a dominant boreal
998 tree species (Picea mariana) in the face of rapid climate change. Canadian Journal of Forest
999 Research. https://doi.org/10.1139/cjfr-2020-0188
1000 Sohn, J.A., Brooks, J.R., Bauhus, J., Kohler, M., Kolb, T.E., McDowell, N.G., 2014. Unthinned slow-growing
1001 ponderosa pine (*Pinus ponderosa*) trees contain muted isotopic signals in tree rings as compared
1002 to thinned trees. Trees 28, 1035–1051. https://doi.org/10.1007/s00468-014-1016-z
1003 Sohn, J.A., Kohler, M., Gessler, A., Bauhus, J., 2012. Interactions of thinning and stem height on the
1004 drought response of radial stem growth and isotopic composition of Norway spruce (*Picea*
1005 *abies*). Tree Physiol 32, 1199–1213. https://doi.org/10.1093/treephys/tps077
1006 Sohn, J.A., Saha, S., Bauhus, J., 2016. Potential of forest thinning to mitigate drought stress: A meta-
1007 analysis. For. Ecol. Manag., Special section: Drought and US Forests: Impacts and Potential
1008 Management Responses 380, 261–273. https://doi.org/10.1016/j.foreco.2016.07.046
1009 Soja, A.J., Tchebakova, N.M., French, N.H.F., Flannigan, M.D., Shugart, H.H., Stocks, B.J., Sukhinin, A.I.,
1010 Parfenova, E.I., Chapin, F.S., Stackhouse, P.W., 2007. Climate-induced boreal forest change:
1011 Predictions versus current observations. Glob Planet Change, Northern Eurasia Regional Climate
1012 and Environmental Change 56, 274–296. https://doi.org/10.1016/j.gloplacha.2006.07.028
1013 Sternberg, L. da S.L.O., 2009. Oxygen stable isotope ratios of tree-ring cellulose: the next phase of
1014 understanding. New Phytol. 181, 553–562. https://doi.org/10.1111/j.1469-8137.2008.02661.x
1015 Stralberg, D., Arseneault, D., Baltzer, J.L., Barber, Q.E., Bayne, E.M., Boulanger, Y., Brown, C.D., Cooke,
1016 H.A., Devito, K., Edwards, J., Estevo, C.A., Flynn, N., Frelich, L.E., Hogg, E.H., Johnston, M., Logan,
1017 T., Matsuoka, S.M., Moore, P., Morelli, T.L., Morissette, J.L., Nelson, E.A., Nenzén, H., Nielsen,
1018 S.E., Parisien, M.-A., Pedlar, J.H., Price, D.T., Schmiegelow, F.K., Slattery, S.M., Sonnentag, O.,
1019 Thompson, D.K., Whitman, E., 2020. Climate-change refugia in boreal North America: what,
1020 where, and for how long? Front Ecol Environ 18, 261–270. https://doi.org/10.1002/fee.2188
1021 Sun, S., He, C., Qiu, L., Li, C., Zhang, J., Meng, P., 2018. Stable isotope analysis reveals prolonged drought
1022 stress in poplar plantation mortality of the Three-North Shelter Forest in Northern China. Agric
1023 For Meteorol 252, 39–48. https://doi.org/10.1016/j.agrformet.2017.12.264

Tang, K., Feng, X., 2001. The effect of soil hydrology on the oxygen and hydrogen isotopic compositions of plants' source water. Earth Planet. Sci. Lett. 185, 355–367. https://doi.org/10.1016/S0012-821X(00)00385-X

Tardieu, F., Simonneau, T., 1998. Variability among species of stomatal control under fluctuating soil water status and evaporative demand: modelling isohydric and anisohydric behaviours. J Exp Bot 49, 419–432. https://doi.org/10.1093/jxb/49.Special_Issue.419

Tissier, J., Lambs, L., Peltier, J.-P., Marigo, G., 2004. Relationships between hydraulic traits and habitat preference for six *Acer* species occurring in the French Alps. Ann. For. Sci. 61, 81–86. https://doi.org/10.1051/forest:2003087

Urban, J., Ingwers, M.W., McGuire, M.A., Teskey, R.O., 2017. Increase in leaf temperature opens stomata and decouples net photosynthesis from stomatal conductance in *Pinus taeda* and *Populus deltoides x nigra*. J Exp Bot 68, 1757–1767. https://doi.org/10.1093/jxb/erx052

Vaganov, E.A., Hughes, M.K., Kirdyanov, A.V., Schweingruber, F.H., Silkin, P.P., 1999. Influence of snowfall and melt timing on tree growth in subarctic Eurasia. Nature 400, 149–151. https://doi.org/10.1038/22087

Verbyla, D., 2015. Remote sensing of interannual boreal forest NDVI in relation to climatic conditions in interior Alaska. Environ. Res. Lett. 10, 125016. https://doi.org/10.1088/1748-9326/10/12/125016

Vicente-Serrano, S.M., Lopez-Moreno, J.-I., Beguería, S., Lorenzo-Lacruz, J., Sanchez-Lorenzo, A., García-Ruiz, J.M., Azorin-Molina, C., Morán-Tejeda, E., Revuelto, J., Trigo, R., Coelho, F., Espejo, F., 2014. Evidence of increasing drought severity caused by temperature rise in southern Europe. Environ. Res. Lett. 9, 044001. https://doi.org/10.1088/1748-9326/9/4/044001

Walker, X.J., Mack, M.C., Johnstone, J.F., 2015. Stable carbon isotope analysis reveals widespread drought stress in boreal black spruce forests. Glob Chang Biol 21, 3102–3113. https://doi.org/10.1111/gcb.12893

Way, D.A., Sage, R.F., 2008. Elevated growth temperatures reduce the carbon gain of black spruce [*Picea mariana* (Mill.) B.S.P.]. Glob Chang Biol 14, 624–636. https://doi.org/10.1111/j.1365-2486.2007.01513.x

Willeit, M., Ganopolski, A., Calov, R., Brovkin, V., 2019. Mid-Pleistocene transition in glacial cycles explained by declining CO_2 and regolith removal. Sci. Adv. 5, eaav7337. https://doi.org/10.1126/sciadv.aav7337

Williams, A.P., Allen, C.D., Macalady, A.K., Griffin, D., Woodhouse, C.A., Meko, D.M., Swetnam, T.W., Rauscher, S.A., Seager, R., Grissino-Mayer, H.D., Dean, J.S., Cook, E.R., Gangodagamage, C., Cai, M., McDowell, N.G., 2013. Temperature as a potent driver of regional forest drought stress and tree mortality. Nat Clim Chang 3, 292–297. https://doi.org/10.1038/nclimate1693

Wu, G., Guan, K., Li, Y., Novick, K.A., Feng, X., McDowell, N.G., Konings, A., Thompson, S.E., Kimball, J.S., De Kauwe, M., Ainsworth, E.A., Jiang, C., 2020. Assessing and interpreting the interannual variability of plant iso/anisohydry at species and ecosystem levels.

Xu, G., Liu, X., Sun, W., Szejner, P., Zeng, X., Yoshimura, K., Trouet, V., 2020. Seasonal divergence between soil water availability and atmospheric moisture recorded in intra-annual tree-ring $\delta^{18}O$ extremes. Environ. Res. Lett. https://doi.org/10.1088/1748-9326/ab9792

Yoshimura, K., Kanamitsu, M., Noone, D., Oki, T., 2008. Historical isotope simulation using Reanalysis atmospheric data. Journal of Geophysical Research: Atmospheres 113. https://doi.org/10.1029/2008JD010074

Yuan, W., Zheng, Y., Piao, S., Ciais, P., Lombardozzi, D., Wang, Y., Ryu, Y., Chen, G., Dong, W., Hu, Z., Jain, A.K., Jiang, C., Kato, E., Li, S., Lienert, S., Liu, S., Nabel, J.E.M.S., Qin, Z., Quine, T., Sitch, S., Smith, W.K., Wang, F., Wu, C., Xiao, Z., Yang, S., 2019. Increased atmospheric vapor pressure deficit

reduces global vegetation growth. Sci. Adv. 5, eaax1396.
https://doi.org/10.1126/sciadv.aax1396